Master's thesis

NTNU
Norwegian University of Science and Technology
Faculty of Natural Sciences
Department of Physics

Sophie Karin Helene Furu Nord

# *In vitro* studies of ROR1 knockdown effects in hypoxic prostate cancer cells

Master's thesis in Applied Physics and Mathematics
Supervisor: Kathrine Røe Redalen
June 2023

NTNU
Norwegian University of
Science and Technology

Sophie Karin Helene Furu Nord

# *In vitro* studies of ROR1 knockdown effects in hypoxic prostate cancer cells

Master's thesis in Applied Physics and Mathematics
Supervisor: Kathrine Røe Redalen
June 2023

Norwegian University of Science and Technology
Faculty of Natural Sciences
Department of Physics

NTNU
Norwegian University of
Science and Technology

# Abstract

**Background**
Most solid tumors contain hypoxic regions, which are associated with resistance to cancer treatment and poor prognosis. Copper-64 (Cu-64) radiopharmaceuticals are emerging as theranostic agents in oncology, for simultaneous diagnosis and treatment of cancer, especially in targeted radionuclide therapy (TRT) of hypoxic tumors. Elesclomol (ES) is an anticancer drug that forms a strong complex with Cu(II), and has previously been investigated for its antiproliferative capacity as a single agent. The theranostic agent $^{64}$Cu-ES has exhibited promising therapeutic effects in hypoxic cancer cells. This appears to be due to decreased activity of receptor tyrosine kinase-like orphan receptor 1 (ROR1). ROR1 is a transmembrane receptor involved in cell signaling, particularly as a co-receptor for Wnt signaling. This protein has low expression in healthy tissue of human adults. However, it has been observed to be highly expressed in many types of malignant tumors, particularly in prostate cancer, and increased ROR1 activity has been seen in hypoxia. However, the effects of ROR1 in cancer are not well understood. Therefore, this study aimed to investigate the *in vitro* effects of ROR1 knockdown (KD) on metabolic activity and cell survival after irradiation in a prostate cancer cell line under normoxic and hypoxic conditions.

**Methods**
A 22Rv1 prostate cancer cell line was maintained in RPMI-1640 medium supplemented with fetal bovine serum (10%) and penicillin at 37°C and 5% $CO_2$. The cells were incubated in normoxic (21% $O_2$) and hypoxic ($O_2 < 1\%$) conditions for four hours prior to and four hours after treatment, in order to create hypoxic conditions in the cells. An anaerobic container was used for hypoxic incubation of the cells. ROR1 KD was done by transfection with the use of small interfering RNA (siRNA) and lipofectamine. To confirm ROR1 KD, cell lysates for Western blotting (WB) with a ROR1 antibody were prepared from hypoxic and normoxic cells. The metabolic activity of cells after ROR1 KD was examined by the XTT assay, and the cell survival after treatment with 0, 2, 4 and 6 Gy of ionizing radiation was examined using the clonogenic survival assay.

**Results**
Reduced metabolic activity and cell survival after irradiation was seen in 22Rv1 cells with ROR1 KD compared to control cells. This effect was greater in hypoxic conditions compared to normoxic conditions. Metabolic activity was reduced by 31% in hypoxic cells with ROR1 KD compared to the hypoxic control, and by 9% in normoxic cells with ROR1 KD compared to the normoxic control. Cell survival decreased in a dose-dependent manner after irradiation, with the hypoxic control having the highest survival for all irradiation doses. The largest differences in survival were seen for the highest dose of 6 Gy, where a 43% decrease in survival was observed in the hypoxic cells with ROR1 KD compared to the hypoxic control, and a 28% decrease in survival was observed in the normoxic cells with ROR1 KD compared to the normoxic control. Due to technical challenges, WB did not validate ROR1 KD, however, KD was assumed to be successful due to the changes in metabolic activity and cell survival observed in attempted ROR1 KD cells by the XTT and clonogenic survival assays.

**Conclusion**
ROR1 KD reduced the metabolic activity and cell survival following treatment with ionizing radiation in a prostate cancer cell line. Cell survival was decreased in a dose-dependent manner after irradiation. The effects of ROR1 KD were greatest in hypoxic conditions. The results of the study strengthened the hypothesis that the increased therapeutic effects of $^{64}$Cu-ES is linked to reduced ROR1 activity, and supports a further investigation of the role of ROR1 in therapeutic response to $^{64}$Cu-ES.

# Sammendrag

**Bakgrunn**
De fleste kreftsvulster inneholder hypoksiske områder, som er assosiert med resistans mot kreftbehandling og dårlig prognose. Kobber-64 (Cu-64) radiofarmaka har vokst frem som et teranostisk legemiddel i onkologi, for simultan diagnose og behandling av kreft, spesielt i målrettet radionuklidbehandling av hypoksiske kreftsvulster. Elesclomol (ES) er legemiddel mot kreft som danner et sterkt kompleks med Cu(II), og har tidligere blitt undersøkt for sine antiproliferative egenskaper som et enkeltstående legemiddel. Det teranostiske legemiddelet $^{64}$Cu-ES has vist lovende behandlingseffekt i hypoksiske kreftceller. Dette ser ut til å være grunnet nedsatt aktivitet av reseptor tyrosin kinase-liknenede orphan receptor 1 (ROR1). ROR1 er en transmembranreseptor involvert i cellulær signaloverføring, spesielt som en koreseptor for Wnt-signaler. Dette proteinet er lite uttrykt i friskt vev hos voksne mennesker. Det har imidlertid blitt observert til å ha høyt uttrykk i mange former for ondartede svulster, og forhøyet aktivitet av ROR1 har blitt observert i hypoksi. Man har imidlertid liten forståelse for effekten av ROR1 i kreft. Av den grunn hadde denne studien til hensikt å undersøke effekter *in vitro* av ROR1 knockdown (KD) på metabolsk aktivitet og celleoverlevelse etter bestråling i en cellelinje for prostatakreft.

**Metoder**
En 22Rv1 cellelinje for prostatakreft ble opprettholdt i RPMI-1640 medium supplementert med fetal bovine serum (10%) og pencillin ved 37°C og 5% $CO_2$. Cellene ble inkubert i normoksiske (21% $O_2$) og hypoksiske ($O_2 < 1\%$) forhold i fire timer før og fire timer etter behandling, med den hensikt å skape hypoksiske forhold i cellene. En anaerobisk beholder ble brukt til hypoksisk inkubasjon av cellene. ROR1 KD ble gjort ved transfeksjon ved bruk av små interferende RNA-molekyler (siRNA) og lipofektamin. For å bekrefte ROR1 KD ble cellelysater for bruk i Western blotting (WB) med et ROR1 antistoff laget av hypoksiske og normoksiske celler. Den metabolske aktiviteten til cellene etter ROR1 KD ble undersøkt med XTT-assay, og celleoverlevelse etter behandling med 0, 2, 4, og 6 Gy ioniserende stråling ble undersøkt ved bruk av klonogent overlevelses-assay.

**Resultater**
Redusert metabolsk aktivitet og celleoverlevelse etter bestråling ble observert i 22Rv1-celler med ROR1 KD, sammenliknet med kontroll-celler. Denne effekten var større i hypoksiske forhold sammenlikned med normoksiske forhold. Metabolsk aktivitet ble resuert med 31% i hypoksiske celler med ROR1 KD sammenliknet med de hypoksiske kontroll-cellene, og 9% i normoksiske celler med ROR1 KD sammenliknet med de normoksiske kontroll-cellene. Dose-avhengig reduksjon i celleoverlevelse ble observert etter bestråling, med høyest overlevelse for de hypoksiske kontroll-cellene for alle strålingsdoser. Den største forskjellen i overlevelse ble observert ved den høyeste dosen av 6 Gy, hvor en 43% reduksjon i overlevelse ble observert i de hypoksiske cellene med ROR1 KD sammenliknet med de hypoksiske kontroll-cellene, og en 28% reduksjon i overlevelse ble observert i de normoksiske cellene med ROR1 KD sammenliknet med de normoksiske kontroll-cellene. På grunn av tekniske utfordringer ble ikke ROR1 KD validert ved WB. Likevel ble det antatt at KD var vellykket på grunn av endringene i metabolsk aktivitet og celleoverlevelse observert i celler med forsøkt ROR1 KD ved XTT- og klonogent overlevelses-assay.

**Konklusjon**
ROR1 KD reduserte metabolsk aktivitet og celleoverlevelse etter behandling med ioniserende stråling i en cellelinje for prostatakreft. Celleoverlevelse ble redusert på en dose-avhengig måte etter bestråling. Effektene av ROR1 KD var størst i hypoksiske forhold. Resultatene fra studien styrket hypotesen om at den økte behandlingseffekten av $^{64}$Cu-ES har sammenheng med redusert aktivitet av ROR1, og støtter videre undersøkelser av rollen til ROR1 i den økte behandlingseffekten av $^{64}$Cu-ES.

# Preface

This thesis is part of my Master's degree in Applied Physics and Mathematics with specialization in Biophysics and Medical Technology at the Norwegian University of Science and Technology (NTNU), Trondheim, Norway. The project was carried out at the Department of Physics during the spring semester of 2023.

I would like to thank my supervisor Kathrine for allowing me to participate in this exciting project. Thank you for all your support and feedback, for always being available for questions, and for valuable insight into the discussion of this project. Additionally, I would like to thank Tengzhi for accompanying me in the lab and teaching me how to perform many of the experiments in this project.

Finally, I would like to thank my family and friends for all your help and support throughout my studies.

# Table of Contents

# List of Figures

# List of Tables

# Abbreviations

**AE** Auger electron

**CTR-1** Copper transporter 1

**DNA** Deoxyribonucleic acid

**DSB** Double strand break

**EC** Electron capture

**ES** Elesclomol

**ETC** Electron transport chain

**HIF** Hypoxia-inducible factor

**IC** Internal conversion

**KD** Knockdown

**LET** Linear energy transfer

**OER** Oxygen enhancement ratio

**PE** Plating efficiency

**PET** Positron emission tomography

**$pO_2$** Oxygen partial pressure

**PTK** Protein tyrosine kinase

**PTM** Post-translational modification

**ROR** Receptor tyrosine-kinase like orphan receptor

**ROS** Reactive oxygen species

**RTK** Receptor tyrosine kinase

**siRNA** small interfering ribonucleic acid

**SPECT** Single-photon emission computed tomography

**SSB** Single strand break

**TRT** Targeted radionuclide therapy

**VHL** von Hippel-Lindau

**WB** Western blotting

# 1 Introduction

Cancer is a complex disease that is a leading cause of death worldwide, accounting for nearly 10 million deaths in 2020. The incidence of cancer continues to rise, with 19.3 million new cases in 2020, and is expected to further increase in the coming years [1]. Despite this, advancements in cancer research, diagnosis and treatment has lead to improved survival rates for cancer patients [2], who now have a greater number of more effective and less toxic therapeutic options than ever before. In order to further improve cancer diagnostics and treatment, it is important to gain a complete understanding of the underlying cellular and molecular mechanisms governing tumor cell interactions with their microenvironment [3].

Most solid tumors contain hypoxic regions, which are tissue regions with low oxygen concentrations. These areas develop because the rapid growth of the tumor outpaces the development of blood vessels to supply oxygen, and causes abnormally shaped vasculature with impaired blood flow. Hypoxic tumors are more aggressive and metastatic than normal tumors, and are resistant to conventional cancer treatments such as radiotherapy and chemotherapy [4]. Therefore, hypoxic tumors are linked to poor patient outcomes [5, 6, 7]. Given the biological problems assicoated with tumor hypoxia, improving techniques for diagnosis and treatment of these types of tumors is of great importance.

In recent years, there has been a growing interest in targeted radionuclide therapy (TRT) as treatment for various cancers. This method uses radiolabeled cancer cell-specific molecules to deliver radiation to cancer cells. This stands in contrast to conventional cancer treatments such as surgery, chemotherapy, and radiotherapy, which are non-selective and therefore cause damage to healthy cells in addition to cancer cells.

Furthermore, in the field of nuclear medicine, there is an increasing focus on combining imaging and therapy applications. This rapidly growing field relies on "theranostic" agents, which is a class of drugs that can be used in both diagnosis and treatment of medical conditions. Theranostics has emerged as an important field in personalized medicine, as it allows for the customization of treatment based on an individual's unique genetic or molecular profile [8]. In particular, copper-64 (Cu-64) is a radionuclide that has gained significant attention in recent years due to its unique properties as a theranostic tool in nuclear medicine. As a radiopharmaceutica, Cu-64 has the ability to emit positrons for imaging by Positron Emission Tomography (PET), and $\beta$ particles for internal radiotherapy. During decay, Cu-64 also generates a cascade of Auger electrons (AEs), which have a high linear energy transfer (LET) and can overcome the radioresistance of hypoxic cancer cells [9, 10].

A commonly used theranostic tracer for hypoxic tumors today is $^{64}$Cu-diacetyl-bis(N(4)- methyl-thiosemicarbazone) ($^{64}$Cu-ATSM), due to its selectivity for hypoxic tissue. This tracer has been used as a diagnostic agent for PET imaging, in addition to being effective in TRT of cancer cells both *in vitro* [11] and *in vivo* [12]. However, the hypoxic selectivity of this tracer has been shown to diminish in prostate cancer cell lines [13, 14], indicating that $^{64}$Cu-ATSM is not ideal for theranostic use in this type of cancer.

Elesclomol (ES) is an anticancer drug that has been shown to exhibit significant toxicity to cancer cells [15]. This drug targets mitochondrial metabolism, which has been observed to be higher in cancer cells compared to healthy cells [16], and the survival and drug resistance of cancer cells rely heavily on energy provided by mitochondrial metabolism [17]. ES forms a strong complex with Cu(II), and the novel radionuclide complex $^{64}$Cu-ES has shown antiproliferative capacity [18]. Upon internalization, ES transports copper into the mitochondria of the cell. Enhanced levels of copper in the mitochondria can cause cell damage and death [15]. Additionally, Kam et al. studied the effects of ionizing radiation on mitochondria, and found that mitochondria are more susceptible to ionizing radiaiton than the cell nucleus [19]. Consequently, $^{64}$Cu-ES arises as a possible theranostic agent.

In the master thesis by M. Lystad, the *in vitro* therapeutic effects of the theranostic agents $^{64}$Cu-ATSM and $^{64}$Cu-ES were studied in prostate cancer cells [20]. Cells treated with $^{64}$Cu-ES showed a significantly larger decreased in survival than cells treated with $^{64}$Cu-ATSM. $^{64}$Cu-ES showed

strong therapeutic effects, both in terms of clonogenic cell survival and metabolic activity. This appeared to be attributed especially to a decrease in the activity of the protein tyrosine kinase (PTK) receptor ROR1. ROR1 is a transmembrane receptor belonging to the ROR subfamily of PTK receptors, but its cellular role is still poorly understood. Studies have demonstrated an important role of ROR1 in oncogenesis by activation of cell survival signaling events, particularly as a co-receptor for the non-canonical Wnt signaling pathway [21, 22]. This pathway has been implicated as an important contributor to prostate cancer progression [23], and high levels of ROR1 expression has been reported in prostate cancer [24].

Additionally, the study by Lystad indicated increased activation of ROR1 in hypoxic compared to normoxic prostate cancer cells [20]. This activation was also decreased after treatment with $^{64}$Cu-ATSM and $^{64}$Cu-ES. The increased activation of ROR1 under hypoxia is supported by Isomura et al., who investigated the role of ROR1 in human lung adenocarcinoma cell lines and found that the kinase activity of ROR1 was needed for regulation of hypoxia-inducible factor 1$\alpha$ (HIF-1$\alpha$) expression [25], which is a protein that aids cells in adaption to hypoxic conditions. They found that knockdown of ROR1 diminished HIF-1$\alpha$ expression in normoxic cells and reduced HIF-1$\alpha$ expression in hypoxic cells. These findings tie expression and activation of ROR1 to cancer cell hypoxia, and indicate that ROR1 may aid cancer cells survival and proliferation in hypoxic conditions. This presents ROR1 as a possible target for TRT in hypoxic tumors. However, the exact role of ROR1 in tumor hypoxia is not yet understood, and further studies are needed to examine the mechanisms of this protein.

This project aimed to investigate the response of the prostate cancer cell line 22Rv1 to inhibition of ROR1, in order to study the role of this protein in cancer survival and proliferation. In particular, the difference in cellular response to ROR1 knockdown (KD) under hypoxic compared to normoxic conditions was studied. This was done in order to elucidate the effect of ROR1 in hypoxic cells, and investigate if the increased effect of $^{64}$Cu-ES in hypoxic prostate cancer cells is linked to reduced activity of ROR1, as indicated by Lystad [20]. For this purpose, *in vitro* cell studies were performed under normoxic and hypoxic conditions. KD of ROR1 was performed by transfection in order to inhibit the ROR1 protein. Western blotting (WB) with an antibody against ROR1 was performed with the aim of validating ROR1 KD. Metabolic activity of the cells after ROR1 KD was investigated by the XTT cell viability and proliferation assay. Additionally, the clonogenic survival of cells with and without ROR1 KD after irradiation with X-rays was assessed with the clonogenic survival assay. The results were analysed and compared in order to examine the effect of ROR1 in hypoxic cells.

# 2 Theory

## 2.1 Cancer

Cancer is a group of more than 100 diseases that develop over time and involves uncontrolled division of the body's cells. Cancer can develop in virtually any tissue in the body, and each type of cancer has its own distinctive characteristics, although the processes that lead to cancer are similar in all types of the disease [26].

The development of cancer results from mutations, deletions, or changes in three groups of genes; activation of oncogenes through mutations that cause the gain of functions, inactivation of tumor suppressor genes through mutations that cause the loss of functions, and the loss of deoxyribonucleic acid (DNA) repair active genes. These mutations may occur spontaneously due to random errors or as a result of external factors such as exposure to chemical agents, viruses or ionizing radiation [27]. However, a single genetic alteration that leads to the activation of an oncogene or loss of a tumor suppressor genes does not, by itself, cause the formation of a solid tumor. Instead, the formation of cancer appears to occur over a period of time, through a multistep process with several genetic alterations [27].

The biological capabilities that tumor cells acquire during the multistep development of human tumors are summarized in the six hallmarks of cancer. These six capabilities provide a solid foundation for understanding the biology of cancer, and consist of sustaining proliferatice signaling, evading growth supressors, activating invasion and metastasis, enabling replicative immortality, inducing angiogenesis, and resisting cell death [28], as shown in Figure 1.

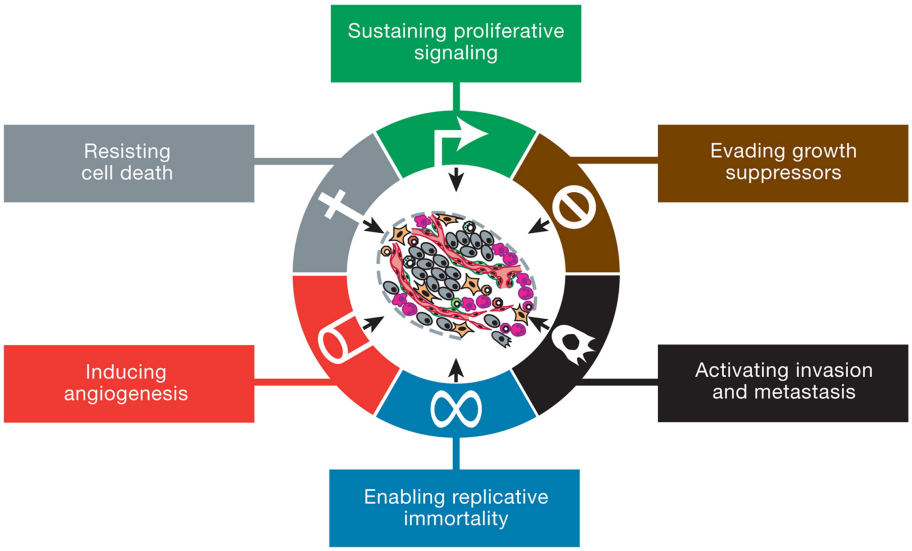


Figure 1: Overview of the 6 hallmarks of cancer; sustaining proliferative signaling, evading growth supressors, activating invasion and metastasis, enabling replicative immortality, inducing angiogenesis, and resisting cell death. Figure from [28].

The six hallmarks of cancer can be summarized as follows:

**Sustaining proliferative signaling**: In normal cells, the production and release of growth-promoting signals is carefully controlled, ensuring a state of balance that allow the cells and tissue to function at their best. In contrast, cancer cells deregulate these signals, leading to uncontrolled growth and proliferation. Sustaining proliferative signaling is arguably the most important trait of cancer cells [28].

**Evading growth suppressors**: In addition to sustaining growth stimulation, cancer cells also bypass systems that negatively regulate cell proliferation through action of tumor suppressor genes. This allows for uncontrolled cancer cell proliferation [28].

**Activating invasion and metastasis**: Cancer cells invade local tissue and spread to remote locations via two distinct processes known as invasion and metastasis. Invasion is the mechanism by which cancer cells expand into nearby environments. Metastasis is the process of tumor cells breaking away from the primary tumor and migrating to a new location to establish a new, secondary tumor [29].

**Enabling replicative immortality**: In order to form macroscopic tumors, cancer cells require the ability of limitless replication through cell division. This stands in contrast to most normal cells, which are only able to pass through the cell cylcle and replicate themselves a finite number of times [28].

**Inducing angiogenesis**: Angiogenesis is the process by which new capillary blood vessels are formed from preexisting functional ones [30]. In normal human tissue, angiogenesis takes place during the first few weeks after fertilization, during the perdiod known as embryogenesis, but after this it is only active in processes such as wound healing and female reproductive cycling. Like normal tissue, tumors require the delivery of nutrients and oxygen. However, in cancer cells, angiogenesis is always active, assisting tumors in sustaining their growth [28].

**Resisting cell death**: The ability of a tumor cell population to increase in number is not only determined by the rate of cell proliferation, but also by the rate of cell death. Apoptosis, which is programmed cell death, is a major source of death in cells, and in normal tissue it is an important mechanism to rid the body of cells that have been damaged beyond repair. Cancer cells have the ability to acquire resistance against apoptosis, enabling uncontrolled growth and division [28].

## 2.2 Nuclear medicine and theranostic agents

Theranostics, a hybrid term fusing the two words therapy and diagnostics, refers to the pairing of diagnostic biomarkes with therapeutic agents, where the two share a specific target in diseased cells or tissues [8]. Nuclear medicine is currently one of the greatest constituents in the field of theranostics, especially with applications in oncology. Theranostics in nuclear medicine refers to the use of radiopharmaceuticals, which are radioactive isotopes that are linked to and guided by molecules such as monoclonal antibodies to bind to targets present on cancer cells but not on normal cells. This allows for nuclear imaging of the site of interest, followed by the use of specifically designed agents for delivery of ionizing radiation to cancer cells [8]. When the radioisotope breaks down by radioactive decay, radiation is emitted, which can damage the DNA the cancer cells and cause them to die. In contrast to external radiotherapy, where the radiation source is placed outside the body of the patient, the maximum dose is not limited by normal tissue complications when using radiopharmaceuticals, as the radiation does not have to go through normal tissue before reaching the cancer cells [31]. Cancer therapy by the use of radioisotopes is not a new phenomenon, as radioactive iodine has been used to treat some types of thyroid cancer since the 1940s, by utilizing the ability of iodine to accumulate naturally in the thyroid [31]. However, it is only recently that serious studies of the use of other types of radiopharmaceuticals have been initiated.

## 2.3 Radioactive decay

This section is adapted from Introductory Nuclear Physics by K. Krane [32].

Radioactivity refers to the process where a nucleus of a substance spontaneously emits radiation, and the state of the nucleus is changed [33]. The resulting nucleus, called the daughter nucleus, will have a lower mass and energy than the decaying mother nucleus, and is more stable. Such decays are statistical in nature, and the probability of decay in a unit time of a nucleus in a sample of N nuclei is described by the decay constant of that particular nuclear species,

$$\lambda = -\frac{(dN/dt)}{N}, \tag{1}$$

where $\lambda$ is the decay constant and N is the number of nuclei present in the sample at time $t$. dN

is then the number of decaying nuclei in a time dt. The probability $\lambda$ is assumed to be constant, regardless of the age of the atom. Integration of Equation 1 gives the exponential law of radioactive decay,

$$N(t) = N_0 e^{-\lambda t}, \tag{2}$$

which describes the number of radioactive nuclei $N(t)$ present in a sample at time $t$, which depends on the initial number of radioactive nuclei, $N_0$, in the sample at time $t = 0$, in addition to $\lambda$ and $t$.

The half-life, $t_{1/2}$, of a radioactive sample is the time necessary for half of the nuclei in the sample to decay. This time is found by setting Equation 2 equal to $N/2$ and solving for $t$, which gives

$$t_{1/2} = \frac{ln(2)}{\lambda}. \tag{3}$$

The activity of a sample of radioactive nuclei is defined as the rate at which decays occur in the sample;

$$A(t) \equiv \lambda N(t) = A_0 e^{-\lambda t}, \tag{4}$$

where $A_0 = \lambda N_0$ is the activity at time $t = 0$. The SI unit for radioactivity is the Becquerel (Bq), equal to one decay per second.

There are three primary ways through which a nucleus can decay; alpha, beta and gamma emission.

### 2.3.1 Alpha, beta and gamma decay

During $\alpha$ decay, the decaying nucleus emits an $\alpha$ particle, which is the nucleus of a helium, ${}^4_2\mathrm{He}_2$, atom. The $\alpha$ particle is chosen for emission because it is a very stable and tightly bound structure, and therefore the kinetic energy released in the decay is maximized. Alpha emission is a Coulomb repulsion effect and many heavy nuclei decay through this type of emission [34]. The spontaneous emission of an $\alpha$ particle can be represented by

$${}^{\mathrm{A}}_{\mathrm{Z}}\mathrm{X}_{\mathrm{N}} \rightarrow {}^{\mathrm{A-4}}_{\mathrm{Z-2}}X'_{\mathrm{N-2}} + \alpha, \tag{5}$$

with $X$ the mother nucleus, $X'$ the daughter nucleus, $Z$ atomic (proton) number, $A$ mass number and $N$ neutron number of the mother nucleus. The energy of the emitted $\alpha$ particle equals the difference in mass energy between the initial and final state. Due to it's large mass, the $\alpha$ particles is the least penetrative of radioactive emissions. It can be utilized in therapeutic nuclear medicine applications to kill cancer cells.

$\beta$ decay happens when a nucleus corrects a proton or neutron excess by directly converting a proton into a neutron or vice-versa [33]. This process can occur in three different ways. The first process is known as negative $\beta$ decay ($\beta^-$), where an ordinary electron is created and emitted together with an antineutrino,

$$n \rightarrow p + e^- + \overline{\nu}.$$

The second process is positive $\beta$ decay ($\beta^+$), involving creation and emission of a positively charged electron (positron) together with a neutrino,

$$p \rightarrow n + e^+ + \nu.$$

The third process is electron capture (EC), where an atomic electron that strays too close to the nucleus is absorbed and a proton is converted into a neutron,

$$p + e^- \rightarrow n + \nu.$$

In contrast to $\alpha$ particles, the emitted $\beta$ particles have a continuous range of energies, from zero up to the energy difference of the initial and final states [35]. This is due to the reaction energy being split between the $\beta$ particle and the neutrino/antineutrino. $\beta^+$ decay is used in diagnostic nuclear medicine applications through positron emission tomography (PET). $\beta^-$ decay is used in therapeutic nuclear medicine applications, such as in brachytherapy, where emissions from a radioactive source is used for cancer treatment.

Radioactive $\gamma$ emissions are photons of high energy which are emitted when an atomic nucleus in an excited state decays to a lower energy state [33]. The energy of the $\gamma$ photon equals the energy difference between the two states. $\gamma$ decay often follows $\alpha$ and $\beta$ decay, as these decays types often leave the daughter nucleus in an excited state. The half-lives of $\gamma$ emissions are usually quite short, generally less than $10^{-9}$s. This type of decay competes with a non-radioactive process called internal conversion (IC), where an unstable nucleus is de-excited by transferring energy directly to an atomic electron, which is kicked out of the atom. $\gamma$ decay is utilized in nuclear medicine applications through single-photon emission computed tomograpy (SPECT) imaging and radiotherapy, where the radiation is used to kill cancer cells. IC is undesirable in nuclear imaging as it increases the dose given to the patient. It can, however, be utilized in therapeutic applications.

### 2.3.2 Auger electrons

Auger electrons (AEs) are low energy electrons emitted by radionuclides that decay by EC or IC [36]. When a nucleus captures an inner orbital (K-shell) electron in EC, a primary electron vacancy is left in the atom. This vacancy is filled by a lower energy electron from a higher orbital. The energy released in the process can cause the emission of a characteristic X-ray photon, with energy equal to the difference in binding energy between the two orbitals. Alternatively, the difference in electronic binding energy is transferred to a lower energy electron in a higher orbital, which is ejected from the atom as an AE. For IC, a primary electron vacancy is left as the unstable nucleus transfers energy to an inner orbital electron, which is ejected from the atom. This primary electron vacancy can be filled by a higher orbit electron, creating a characteristic X-ray or an AE. An illustration of the generation of AEs is shown in Figure 2.

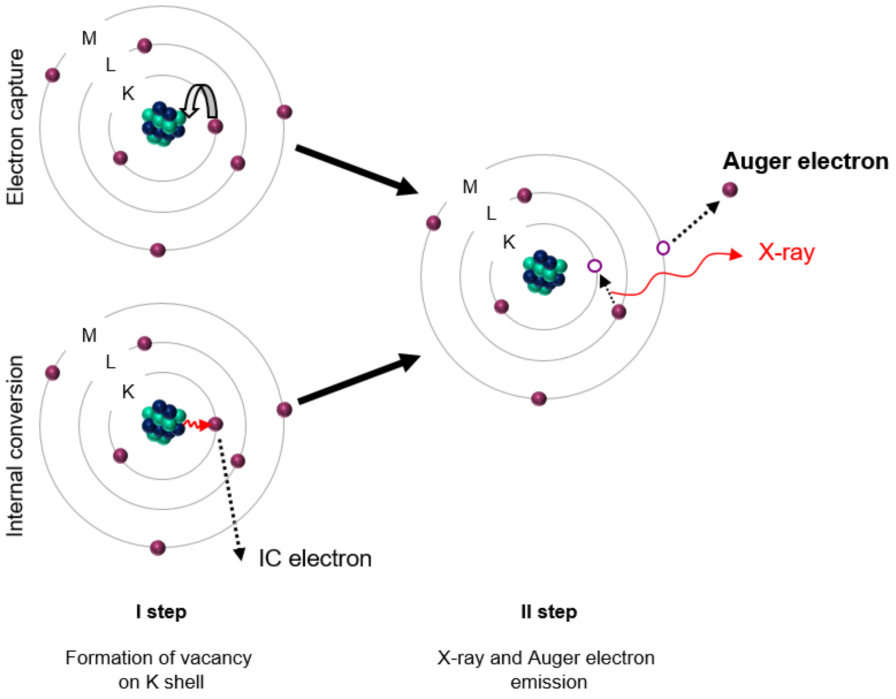


Figure 2: Generation of auger electrons. Step I: A primary electron vacancy is created during EC or IC. Step II: The vacancy is filled by a higher orbit electron, and the excess energy is released as either a characteristic X-ray or an AE. Figure from [37].

The majority of AEs have low energy, less than 25 keV, which is deposited over short ($10^{-9} - 10^{-6}$ m) distances in tissue [36]. The extremely short range means that the AEs transfer a large amount of energy per distance traveled. This makes them attractive for radiation treatment of cancer, as long as they are emitted close to sensitive targets of the cancer cells such as DNA and the cell membrane [36].

### 2.3.3 Radioactive decay of Cu-64

Copper-64 (Cu-64) is a radioactive isotope which properties make it suitable as a theranostic agent. The decay scheme of Cu-64 is shown in Figure 3. It has a half-life of 12.7 hours, and decays to either Zn-64 by $\beta^-$ emission (39.0%), or to Ni-64 by $\beta^+$ emission (17.9%) or EC either straight to the ground state of Ni-64 (42.3%) or to an excited state of Ni-64 (0.47%) followed by a 1.346 MeV $\gamma$ emission to reach the ground state [38]. The decay modes of Cu-64 allows for it to be used in both diagnostic and therapeutic nuclear medicine applications; $\beta^+$ decay makes it suitable as a radiopharmaceutical for PET imaging, while $\beta^-$ and AE emission from EC can be used for cancer treatment through internal radiotherapy.

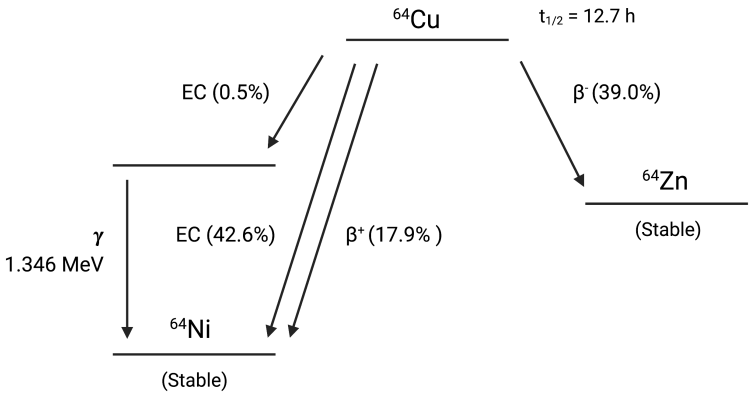


Figure 3: Decay scheme of Cu-64, with a half-life of $t_{1/2} = 12.7$ hours, which decays via 39.0% $\beta^-$, 17.9% $\beta^+$, 43.4% electron capture (EC), and 0.5% $\gamma$ emission.

Additionally, the half-life of Cu-64 makes it convenient for medical applications. With 12.7 hours, it is long enough for the activity of the radiopharmaceutical to remain high during the time needed for it to accumulate in tumor cells and to acquire PET images. At the same time, it is short enough for a substantial number of decays to occur before the substance is excreted from the body when used as a therapeutic agent to deliver dose to the patient.

## 2.4 Biological effects of radiation

This section is adapted from my specialization project [39].

Absorption of energy from radiation in biological material can lead to excitation or ionization of an atom or molecule in the material. Excitation occurs when an electron in an atom or molecule is raised to a higher energy level without being ejected. If the radiation gives off enough energy for the electron to be ejected from the atom or molecule, the process is called ionization. Radiation capable of ionizing atoms or molecules is classified as ionizing radiation, and characterized by local release of large amounts of energy [40]. Ionizing radiation is further classified into directly or indirectly ionizing. Directly ionizing radiation can disrupt the atomic structure of absorbing material, pass directly through it, and cause chemical and biological damage, as long as the individual particles of the radiation have sufficient kinetic energy. Directly ionizing radiations include charged particles, such as protons, electrons and $\alpha$ particles. On the other hand, indirectly ionizing radiation cannot cause chemical and biological damage itself, but instead gives up its energy to fast moving charged particles when it passes through a material. These charged particles are in turn capable of producing chemical and biological damage. High energy electromagnetic radiation, including X-rays and $\gamma$-rays are ionizing [40]. The amount of energy deposited in matter by ionizing radiation per unit mass is quantified by the absorbed dose, D, which is measured in Grey (Gy), where $1\,\mathrm{Gy} = 1\,\mathrm{kg/J}$.

### 2.4.1 Direct and indirect action of radiation

The biological effects of radiation primarily results from damage to DNA [40]. There are two main ways in which radiation can damage DNA, namely through direct and indirect action of radiation, which mechanisms are shown in Figure 4a and b, respectively. Direct action of radiation occurs when radiation absorbed in a biological material interacts directly with the DNA in the cell, causing ionizations that initiate the chain of events that leads to biological damage. Alternatively, the radiation can produce free radicals through interact with other atoms or molecules in the medium, such as water. Free radicals are molecules that are highly reactive because they contain an unpaired electron in an atomic orbital [41], and can therefore cause damage by reacting with other structures in the cell. This process is known as indirect action of radiation.

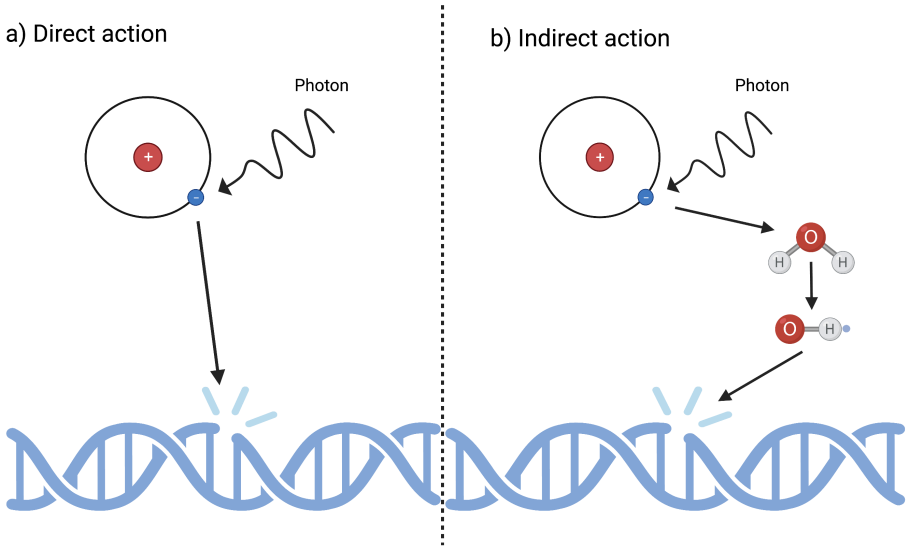


Figure 4: Illustration of a) direct and b) indirect action of radiation, following photon radiation absorption in biological material. An incoming photon ionizes an atom in the material, creating fast moving electrons. These electrons can cause damage to DNA by a) interacting directly with the DNA or b) producing free radicals which highly reactive and can further interact with DNA.

### 2.4.2 DNA strand breaks and linear energy transfer (LET)

DNA is a large molecule with a double helical structure, consisting of two strands of sugar and phosphate groups with nucleotide bases attached. The strands are held together by hydrogen bonds between the bases. When ionizing radiation causes damage to one of the two strands of the DNA helix, it is called a single strand break (SSB). SSBs are of little biological consequence with respect to cell killing, because this type of damage is easily repaired by the cell [42]. If both DNA strands are damaged, but the beaks are well separated along the length of the DNA, repair can again occur easily. However, if breakage occurs close to each other on opposite strands of the DNA, it can lead to a double strand break (DSB), causing the DNA to be cleaved into two pieces. DSBs are belived to be the most serious type of DNA damage, and can lead to cell death or mutations [42].

Ionizations and exciatations that occur in biological material as a consequence of ionizing radiation tend to be localized along the track of individual charged particles, with a pattern that depends on the type of particle involved [43]. Linear energy transfer (LET) is a quantity that describes the energy transferred per unit path length traveled by charged particles in matter. It is defined as $dE/dl$, where $dE$ is the average energy imparted to the medium by a charged particle of specific energy in a traversed distance $dl$. LET is an average quantity and is measured in keV/µm. The LET of a charged particle increases with decreasing energy of the particle. Charged particles are most efficient in causing biological damage for cell killing at an LET of 100 keV/µm, as shown in

Figure 5. This is due to the average separation between ionizing events being approximately 2 nm, which equals the separation between the strands of the DNA double helix. Therefore, radiation with this density of ionization has the highest probability of causing a DSB by the passing of one particle. X-rays, which are more sparsely ionizing than charged particles, have a low probability of causing a DSB by a single particle. Contrarily, particles with a LET higher than 100 keV/µm will cause more ionizations within the diameter of DNA than is necessary for a DSB, and therefore no further biological effects will occur [43].

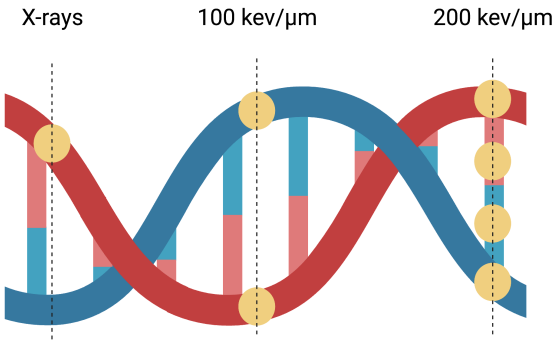


Figure 5: Illustration of the ionization density of different radiations. The most efficient DNA damage is caused by charged particles of linear energy transfer (LET) of 100 keV/µm, because this is approximately the separation distance between the two strands of DNA. X-rays generally have a lower LET, and therefore a lower biological effect. An increase in LET beyond 100 keV/µm will cause a higher ionization density, but no further biological effect.

### 2.4.3 The oxygen effect

Various chemical and pharmacologic substances that modify the biological effect of ionizing radiation have been discovered, and oxygen is the one that has been seen to cause the most dramatic effects. A clear correlations exists between biological damage by ionizing radiation and the presence of oxygen. This correlation is described by the oxygen enhancement ratio (OER), which is the ratio of dose administered to hypoxic and normoxic tissue needed to cause the same biological effect [44]. The OER for indirectly ionizing radiations, such as X- and $\gamma$ rays, has been determined to a value between 2.5 and 3.5. This means that in order to cause the same biological damage to hypoxic and normoxic cells, the dose delivered to hypoxic cells must be approximately 3 times that to normoxic cells. For directly ionizing radiations, such as $\alpha$ particles, the oxygen effect is absent, and the OER equals 1 [44].

There is a general agreement that oxygen affects the biological damage of ionizing radiation through its interaction with free radicals, which are produced by fast charged particles as they move through tissue. Free radicals act through breaking chemical bonds, producing chemical changes, and initiating the chain of events that leads to biological damage [44]. It has been observed that the extent of damage caused by free radicals is dependent on the presence or absence of oxygen. DNA reacts with the free radicals, but if oxygen is not present, the DNA radical can be restored to its reduced form through reaction with a sulfhydryl group, and the DNA damage can be repaired. However, if oxygen is present, the formation of an organic peroxide occurs, which represents a non-restorable form of the DNA. Oxygen is therefore said to "fix" the damage created in DNA by ionizing radiation [44]. Due to this effect, hypoxic tumor cells are more difficult to kill with indirectly ionizing radiation than normoxic tumor cells.

### 2.4.4 Cell death following irradiation

Cell death has different meanings in different contexts, and therefore a precise definition is needed. For differentiated cells that do not proliferate, death can be defined as loss of specific functions. For

proliferating cells, death is defined as loss of ability to sustain proliferation indefinitely. Contrarily, clonogenic cells are defined as surviving cells that have retained their reproductive integrity and can proliferate indefinitely to form a colony. Regarding the treatment of malignant tumors, it is only necessary for the cells to be killed in the way that they are no longer able to proliferate and cause further spreading of the disease [45]. Cells may die through several different processes, however, the main mechanisms by which ionizing radiation cause death of cells is mitotic catastrophe, i.e. death while attempting to divide.

Mitotic catastrophe occurs when a cell is not able to repair the DNA damage caused by radiation before it enters mitosis. This causes failure of cell division leads to mitotic death. Mitotic death may occur in the first or a subsequent cell division following irradiation, and can lead to secondary cell death through either apoptosis, autophagy, necrosis, or senescence.

Apoptosis, also called programmed cell death, is an orderly process in which the cell contents are broken down and separated into several membrane-bound fragments. Irradiated cells that undergo apoptosis die as an immediate consequence of radiation damage, usually within a few hours of radiation. These cells show characteristic morphological changes, such as loss of normal nuclear structure and degradation of DNA [46]. However, loss of apoptotic control is a characteristic mechanism of malignant tumors, as described in Section 2.1, and the extent to which irradiated tumor cells die through apoptosis is highly cell-type dependent [45]. Autophagy is a self-digestive process, where old, damaged, unnecessary, or dysfunctional cell components are broken down within the lysosome of the cell [47]. Necrosis is accidental death due to extreme environmental conditions or stimuli, unlike apoptosis, which is highly regulated [48]. Lastly, senescence is the process by which cells irreversibly stop dividing and enter a state of permanent growth arrest without undergoing cell death [49].

Abundant evidence shows that the primary sensitive site for irradiation-induced cell damage is the DNA located in the nucleus [45]. However, emerging experimental evidence suggests that this is insufficient for describing effects of ionizing radiation outside the nucleus. In particular, the mitochondria provides an interesting target for cancer therapy by ionizing radiation, because it is the only site in the cell except the nucleus that contains DNA, while lacking histone protection [50] and an efficient DNA repair system [51, 52]. Moreover, mitochondria are involved in initiating cell death through apoptosis by caspase activation [53]. Therefore, mitochondria may provide a target for cancer therapy.

## 2.5 Tumor hypoxia

Hypoxia, or low oxygen conditions, is common in a majority of solid malignant tumors. It is caused by an imbalance between oxygen supply and consumption in the cells, when the rapid growth of the tumor outpaces the ability of its existing vasculature to supply nutrients and oxygen [54]. The average oxygen concentration in normal tissue is around 5%, while most tumors exhibit median oxygen levels of less than 2% [55], both much lower than the 21% in air. Hypoxia in tumors can result from two different mechanisms; chronic or acute hypoxia.

Chronic hypoxia is a result of the limited diffusion distance of oxygen through respiring tumor cells. The oxygen is consumed by the tumor cells closest to the capillaries, and tumor cells that lie further away from the capillaries become chronic hypoxic [44], as shown in Figure 6a. In contrast, acute hypoxia results from the temporary closing of a tumor blood vessel due to the deformed vasculature of the tumor. Tumor vasculature lacks smooth muscles and often has incomplete endothelial lining and basement membrane [44]. Acute hypoxia therefore fluctuates over time with the random opening and closing of tumor blood vessels. Figure 6b shows an illustration of acute hypoxia.

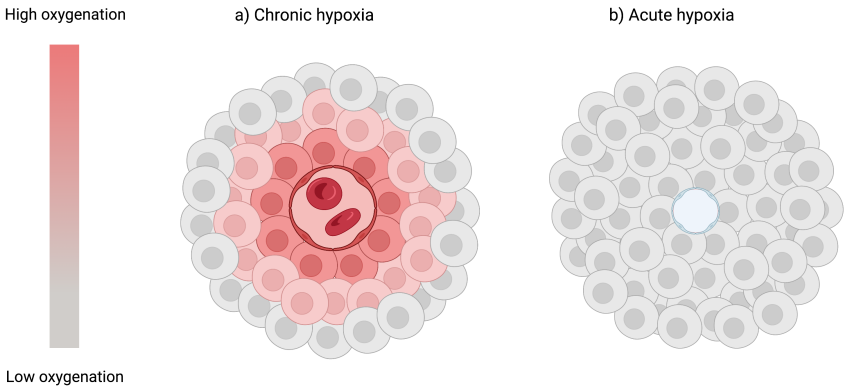


Figure 6: Oxygenation levels of tumor cells under a) chronic hypoxic and b) acute hypoxic conditions. In chronic hypoxia, oxygentation levels decrease with the distance from the tumor blood vessel. In acute hypoxia, all cells in the vicinity of the blood vessel experience low oxygenation.

### 2.5.1 Tumor adaption to hypoxia and hypoxia-inducible factors

Cells experiencing hypoxia can adapt by either increasing the oxygen supply or accommodate to the low oxygen level. Hypoxia-inducible factors (HIFs) are transcription factors that facilitate both oxygen delivery and adaption to low oxygen conditions by regulating the expression of genes that are involved in many important cellular processes, including glucose uptake and metabolism, angiogenesis, cell proliferation, and apoptosis [54].

To date, three HIFs (HIF-1, -2 and -3) have been identified, that regulate transcriptional factors as a response to low oxygen levels. Most hypoxia-inducible genes are expressed due to activity of HIF-1, which concentration in the cells increases exponentially with decreasing oxygen levels, with a half maximal and maximal response at 1.5 - 2% and 0.5% $O_2$, respectively [56]. HIF-1 is a heterodimer complex, consisiting of an oxygen-sensitive $\alpha$-subunit and a constantly expressed $\beta$-subunit. Figure 7 shows how HIF-1$\alpha$ is regulated in normoxic versus hypoxic conditions. In the presence of oxygen, HIF-1$\alpha$ is hydroxylated on two proline residues. This hydroxylation of HIF-1$\alpha$ enables binding to the von Hippel-Lindau (VHL) tumor suppressor protein, which facilitates the destruction of the HIF-1$\alpha$ through binding of ubiquitin groups [54]. Under hypoxic conditions, the hydroxylation of HIF-1$\alpha$ cannot occur due to lack of oxygen. This enables HIF-1$\alpha$ to escape the binding to VHL, and the protein is stabilized. HIF-1$\alpha$ instead binds to HIF-1$\beta$ in the cell nucleus, forming the HIF transcription complex, which promotes transcription of genes involved in tumor growth, angiogenesis and metastasis [54].

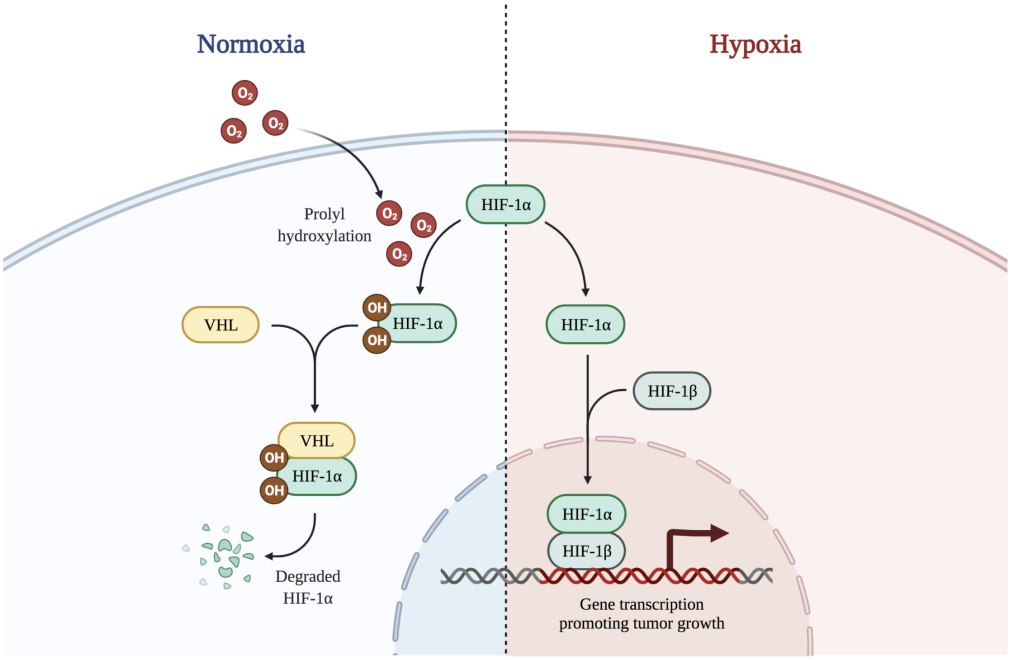


Figure 7: Regulation of hypoxia-inducible factor-1$\alpha$ (HIF-1$\alpha$) under normoxic versus hypoxic conditions. In normoxic conditions, HIF-1$\alpha$ is hydroxylated on two proline residues, which enables the binding of the tumor supressor gene von Hippel-Lindau (VHL). This promotes degradation of HIF-1$\alpha$. Under hypoxic conditions, HIF-1$\alpha$ is stabilized and binds to HIF-1$\beta$ in the cell nucleus, forming the HIF-1 transcriptional complex. This complex promotes transcription of target genes involved in tumor growth, angiogenesis, and metastasis. Figure from [20].

## 2.6 Copper radiopharmaceuticals

Copper is an important nutrient for many biochemical processes, because it functions as a cofactor for enzymes that catalyse redox reactions [57], which are chemical reactions that involves a transfer of electrons between species [58]. These reactions are involved in fundamental metabolic processes, and copper is therefore critical for human growth and development. At the same time, the redox properties of copper makes it potentially toxic in free from, and the uptake and intracellular distribution of this metal is therefore strictly regulated [59].

Uptake of copper from blood is mainly mediated by copper transporter 1 (CTR-1), which is a high-affinity protein that transports copper into the cell. This occurs by Cu(II) being absorbed by albumin and delivered to the extracellular domain of CTR-1. CTR-1 imports copper across the cell membrane and delivers it to chaperone proteins, that further transport it to sites where it is needed, such as the mitochondria [9]. Due to the potentially toxic effects of copper, regulation of CTR-1 is crucial, and the signaling pathways that regulate tumor response to hypoxia and cellular copper transport are correlated [9]. In hypoxic environments, where the HIF-1$\alpha$ subunit is stabilized and toghether with HIF-1$\beta$ forms the HIF-1 transcription complex, as described in Section 2.5.1, alterations in the control of critical cellular functions occur. Notably, copper is required for the activation of HIF-1 through binding of HIF-1$\alpha$ to the hypoxia-responsive element of genes and the formation of the HIF-1 transcriptional complex [60]. Similarly, hypoxia has been shown to stimulate the expression of CTR-1, and several studies have shown the upregulation of CTR-1 in hypoxic tumors [61, 62, 63, 64].

The strict regulation of copper transport has proved to be useful in theranostic applications of copper radiopharmaceuticals in hypoxic tumors. Although the uptake mechanisms of copper are still controversial, there is a consensus that it is related to the redox potential and reactive oxygen species (ROS). ROS which are unstable molecules that easily react with other molecules in the cell, characterizing cells with an hypoxic environment [65]. Hypoxic cells experience oxidative

stress, which involves an increase in the production levels of ROS in the mitochondria of the cell. ROS can reduce intramitochondrial Cu(II) to Cu(I), which, due to the strict regulation mechanisms of copper, causes the metal ion to be irreversibly trapped inside the mitochondria [65]. This trapping only occurs in cells that experience oxidative stress, and is therefore infrequent in normoxic cells. Thus, copper can be used to target hypoxic tumor cells. Furthermore, by using the radioactive copper isotope Cu-64, ionizing radiation can be delivered to the mitochondria of the cancer cells and allow for positron emission tomography (PET). Additionally, Cu-64 allows for simultaneous internal radiotherapy through emission of AEs with high LET, which have the possibility to overcome the radioresistance of hypoxic cells.

$^{64}$Cu-ATSM is a common Cu-64 radiopharmaceutical used for theranostic applications in hypoxic tumors today. The molecule Cu-ATSM is of suitable molecular size and lipophilicity to penetrate cell membrane from the blood stream [66], and radiolabeling with Cu-64 allows for its application in nuclear medicine. When this substance enters hypoxic cells, the radiouclide is trapped in the cell and can cause damage by AE emission [65]. An overwhelming body of literature on Cu-ATSM supports it selectivity in hypoxic tumors. However, recent studies have shown considerable variation in Cu-64 accumulation in different cell lines following incubation with $^{64}$Cu-ATSM. In particluar, Burgman et al. demonstrated a decrease in $^{64}$Cu-ATSM in anoxic and hypoxic prostate cancer cells, in contradiction with models that suggest irreversible trapping under low-oxygen concentration conditions, indicating that this compound may not be ideal for TRT in prostate cancer [13].

Elesclomol (ES) is an anticancer drug that forms a strong complex with copper ions, and the complex Cu-ES has previously been studied for its anti-proliferative capacity [18]. The therapeutic effect of ES on cancer cells is determined by the dependence of cancer on mitochondrial metabolism. Mitochondrial metabolism plays a critical role in tumorgenesis, proliferation, metastasis, and drug resistance [17]. Therefore, targeting mitochondrial metabolism is an effective strategy for cancer suppression. ES is recognized as an inducer of oxidative stress in the mitochondria. It binds to Cu(II) outside of the cell and enters as the complex Cu-ES. It then selectively transports copper to the mitochondria of the cell, where Cu(II) is reduced to Cu(I), followed by generation of ROS. ROS contribute to elevating oxidative stress levels, which, if increased beyond a breaking point, triggers apoptosis in the cell. After dissociation from copper, ES is effluxed from the cell and the process is repeated. Due to cancer cells having already increased oxidative stress level, they are more vulnerable to agents such as ES than normal cells [18].

Additionally, utilizing the radiolabeled $^{64}$Cu-ES, which is administered in a much lower and non-toxic dose than when used as monotherapy, provides further opportunity to target the mitochondria of cancer cells by means of ionizing radiation. A study by Kam et. al examined the effects of ionizing radiation on the mitochondria, and inferred that mitochondria are more susceptible to ionizing radiation than the cell nucleus [19]. The mitochondrial genome contains a higher genetic information density than the nuclear genome. Therefore, damages caused by ionizing radiation that could lead to functional changes are more likely to be found in mitochondrial DNA. Additionally, regions within the mitochondrial DNA could be deleted upon exposure to ionizing radiation, leading to alterations in the function of the electron transport chain (ETC), which is a series of protein complexes involved in redox reactions. Disturbances in these reactions may lead to an increase in ROS generation, which can further damage the DNA [19].

The potential of $^{64}$Cu-ES as a theranostic agent for hypoxic tumors was demonstrated in the master thesis by Lystad [20]. Here, the the effects of $^{64}$Cu-ATSM and $^{64}$Cu-ES on prostate cancer cell lines PC3 and 22RV1 in normoxic and hypoxic conditions were studies, and an increased therapeutic effect of $^{64}$Cu-ES compared to $^{64}$Cu-ATSM was observed. This appeared to be a result of a combination of radiation-induced and chemical-induced cell death. In paricular, the activity of receptor tyrosine kinase-like orphan receptor 1 (ROR1) seemed to be important. However, the exact role of ROR1 in cancer cell survival and proliferation is not yet understood.

## 2.7 Protein tyrosine kinases (PTKs)

Treatment with the theranostic agents $^{64}$Cu-ATSM and $^{64}$Cu-ES has been identified to affect the activity of enzymes known as protein tyrosine kinases (PTKs) [20]. In this section, the mechanisms and roles of these enzymes in cell signaling and carciogenesis will be elucidated.

The functions of proteins involved in biological systems can be modified by a variety of factors. Post-translational modification (PTM) is the modification of amino acid side chains in a protein after biosynthesis [67], which causes a change in the properties of the protein. There are more than 400 types of PTMs affecting many aspects of protein functions. In particular, post-translational phosphorylation, which involves the attachment of a phosphate group to a molecule or ion, is an important reversible regulatory mechanism that plays a key role in the activities of many enzymes, membrane channels, and other proteins in prokaryotic and eukaryotic organisms [67]. This is due to many enzymes and receptors being activated/deactivated by phosphorylation/dephosphorylation [68]. Phosphorylation is mediated by kinases, which are enzymes that transfer a phosphate group from ATP to another protein or molecule. More than one third of all protein phosphorylation occur on the amino acids serine, threonine and tyrosine within the target protein. Protein tyrosin kinases (PTKs) are kinases responsible of phosphorylating tyrosine.

### 2.7.1 The roles of PTKs in cell signaling

PTKs are involved in mediating cell-to-cell communications and controlling a wide range of complex biological functions, including cell growth, differentiation, motility and metabolism [69]. Activation of proteins through tyrosine phosphorylation by PTKs can initiate cellular signals downstream in a cascading manner, or lead to the supression of a signal.

Of 90 tyrosine kinases identified in the human genome, 58 are receptors tyrosin kinases (RTKs). [70]. Most RTKs are single-pass transmembrane proteins. They are composed of an extracellular ligand binding domain, a single transmembrane helix, and an intracellular region containing the tyrosin kinase domain. The activation process of RTKs is shown in Figure 8. Activation is initiated when a receptor-specific ligand binds to the RTK extracellular domain, which cause dimerization of two tyrosine kinase domains. This initiates autophosphorylation of the tyrosine residues, further activating intracellular signaling proteins so that extracellular signals are transduced to the cell interior. These signals can modify gene expression by activation of transcriptional factors or by regulating cell cycle-associated proteins.

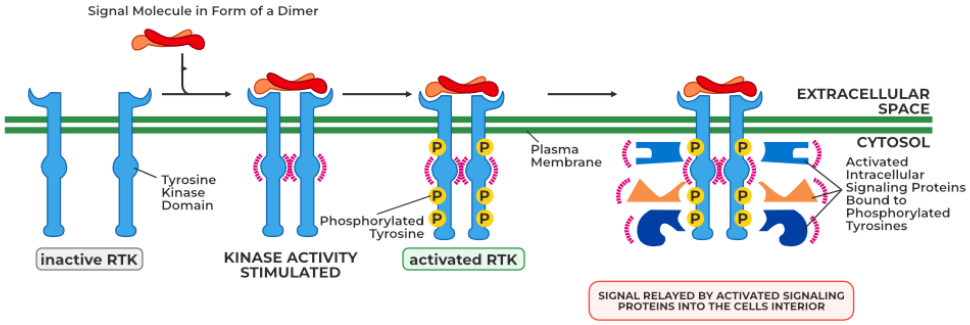


Figure 8: Activation of receptor tyrosine kinases (RTKs) through dimerization in the presence of ligands, which results in kinase activation and phosphorylation of the tyrosine domains. This facilitates binding of signaling proteins to the phosphorylated tyrosine, causing activation of cellular signaling pathways. Figure from [71].

### 2.7.2 PTKs in carciogenesis

Cancer progression and development of treatment resistance is characterized by an alteration of gene expression and the subsequent change in protein expression and functions. These alterations disrupt normal cell function and cause cancer cells to over-proliferate and avoid mechanisms that normally control their survival and migration. Many of the defects driving cancer cell proliferation is linked to signaling pathways that control cell growth, division, death, and motility [72].

In particular, abnormal PTK signaling has been linked to a variety of cancers, as these proteins control the activation of major signaling pathways involved in cellular processes relevant for cancer development [73]. In healthy cells, the level of PTK activation through phosphorylation is tightly regulated. However, genetic mutation and/or prolonged activity of these proteins may inititate and promote carciogenesis. Over half of the identified protein kinome has shown involvement in human cancer, either through mutation or overexpression [73]. For example, mutations in a gene encoding a PTK can cause the protein to be continuously active, leading to a constant growth signal in the cell and uncontrolled cell division. Therefore, PTKs have become an attractive target for cancer treatment. Tyrosine kinase inhibitors (TKIs) are continuously developed, and are currently used in treatment of cancers that show a high expression of certain PTKs [73]. Imatinib, an inhibitor for Abelson (ABL) tyrosin kinase, which is expressed as a deregulated fusion protein in nearly all cases of chronic myeloid leukemia (CLM), was in 2001 the first drug developed by targeting specific protein kinases to treat diseases to be approved by the FDA [74]. Targeting of the epidermal growth factor receptor (EGFR), which is involved in cell growth, has also yielded significant survival benefits for patients with non-small cell lung cancer (NSCLC) [75]. Furthermore, targeting of human epidermal growth factor receptor 2 (HER2), which is found in 15-20% of invasive breast cancer and is considered to be associated with poor differentiation, rapid cell proliferation, lymph node involvement, and resistance to chemotherapy, has significantly improved the outcome of patients with HER2-positive breast cancer [76].

## 2.8 Receptor tyrosine kinase-like orphan receptor 1 (ROR1)

The receptor tyrosine kinase-like orphan receptor (ROR) family is a subfamily of RTKs, and contains two members, ROR1 and ROR2. The ROR subfamily was named "orphan" because for many years their ligands were not identified. It is now known that they are receptors for Wnt family signaling molecules Wnt5a/b and Wnt16, and are involved in signaling through Wnt pathways [21]. ROR1 is an RTK that is imporant for developement during embryogenesis in humans, but minimally expressed in normal, developed tissue. It is however, overexpressed in many types of malignant tumors, and may act as a survival factor for tumor cells.

### 2.8.1 The structure of ROR1

ROR1 is a transmembrane receptor, which contains an extracellular receptor doimain, a transmembrane segment, and a cytoplasmic domain. Figure 9 shows an illustration of the structure of ROR1. The extracellular part consists of an immunoglobulin-like domain (IG), a cystein-rich domain (CRD) and a kringle domain (KD) [21]. Immunoglobulins (Ig), also called antibodies, are molecules that compose a critical part of the immune system. They specifically recognize and bind particular antigenes, such as bacteria or virus, and aid their destruction. Ig-like domains are protein domains that are similar in structure to the domains of immunoglobulins. CRD facilitates $\beta$-catenin-independent Wnt signaling, which will be discussed in the next section, by binding to the Wnt5a ligand [77]. The KD domain mediates interaction of ROR1 with other proteins. The cytoplasmic section of ROR1 includes a tyrosin kinase domain (TKD), two serine/threonine-rich domains (S/T), and a proline-rich domain (PRD). The S/T-rich domain interacts with adaptor proteins, which cause resistance to apoptosis. The proline-rich domain is involved in activation of cell migration and proliferation [21]. Although ROR1 is a member of the PTK family, the function of its tyrosin kinase domain is controversial.

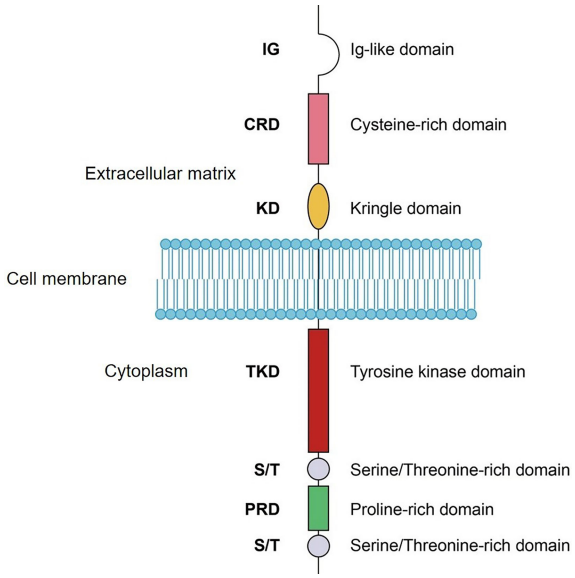


Figure 9: Illustration of the structure of ROR1. Extracellularly, ROR1 contains an immunoglobulin-like domain (IG), a cystein-rich domain (CRD), and a kringle domain (KD). Intracellularly, there is a tyrosin kinase domain (TKD), two serine/threonine-rich domains (S/T), and a proline-rich domain (PRD). Figure from [21].

### 2.8.2 Wnt signaling pathways and ROR1

Wnt signaling pathways compose a group of signal transduction pathways that use Wnt family proteins as ligands. Wnt signaling has been shown to regulate many key cellular processes, and unusual regulation of this pathway has been associated with development of many types of cancer. The Wnt pathways are categorized into the canonical $\beta$-catenin-dependent and non-canonical $\beta$-catenin-independent pathways [21]. The $\beta$-catenin-dependent signaling pathway is activated by some Wnt ligands, including Wnt1, Wnt3a and Wnt8, when they bind to members of the Frizzled receptor family connected to the cell membrane. This stabilizes $\beta$-catenin, which is translocated into the nucleus, where it activates the transcription of target genes involved in regulation of cell proliferation and differentiation [22]. Alternatively, other Wnt ligands such as Wnt5a/b and Wnt16 can initiate signaling via the $\beta$-catenin-independent Wnt/planar cell polarity and Wnt/$Ca^{2+}$ pathways, which activates small GTPases Rho/Rac signaling proteins and protein kinase C (PKC)/calcineurin signaling cascade, respectively [21]. The Wnt $\beta$-catenin independent pathways are know to regulate cell polarity, proliferation, motility, and migration [21], although these pathways are insufficiently studied.

In recent years, it has become apparent that at least one other non-canonical Wnt subpathway exist, namely Wnt/ROR signaling via the ROR family receptors ROR1 and ROR2. Specifically, the ROR proteins activate non-canonical Wnt signaling by binding the Wnt5a ligand. Studies have shown that Wnt5a ligand binding causes autophosphorylation of ROR2, which leads to activation of $\beta$-catenin-independent pathways [78]. Autophosphorylation of ROR1 and the associated downstream signaling network is, however, not well understood. Moreover, when studying the downstream signaling events of the ROR co-receptors by modulating their expression, it should be considered that the downregulation of one of the RORs could trigger upregulation of the other, which may compensate for the loss of the former [22]. For example, ROR1 knockdown (KD) in melanoma was followed by increased expression of ROR2 and Wnt5a, while KD of ROR2 stimulated ROR1 expression [79], confirming a mutual regulation.

In addition to activating cellular responses through the non-canonical $\beta$-catenin independent Wnt pathways alone, ROR1 seems to be a crossroad that can link Wnt signals to other major signaling pathways implicated in important cellular processes [22]. Menck et al. discussed the current knowledge about Wnt/ROR signaling and its crosstalk with other pathways [22], which is summarized in Figure 10. In particular, the PI3K/AKT pathways seems to be closely related to Wnt/ROR1

signaling. This pathway is mediated by the activation of protein kinase B (AKT), and plays a role in cell metabolism, growth, proliferation, and survival. Activation of the pathway is tightly controlled in a multistep process that involves phosphoinositide-3-kinase (PI3K) [80]. Activation of ROR1 has been shown to induce phosphorylation of PI3K and AKT, in addition to the transcription factor cAMP response element-binding protein (CREB)[81, 82, 83, 84, 24]. Ciu et. al. found diminished expression of phosphorylated AKT and CREB in immunodeficient mice injected with metastases derived from ROR1 KD breast cancer cells [85]. ROR1 KD has also been shown to reduce the phosphorylation of AKT and glykogen synthase kinase-3 beta (GSK3$\beta$) [86], which is a regulator of glycogen metabolism. Other pathways activated by Wnt/ROR1 signaling are mitogen-activated protein kinase (MAPK)/extracellular signal-regulated kinase 1/2 (ERK) [81, 87], which is the core of the signaling network involved in regulating growth, development and division of cells [88], signal transducer and activator of transcription 3 (STAT3) [89], a transcription factor that, when activated, is translocated to the nucleus to participate in the transcriptional regulation of DNA [90], and nuclear factor-$\kappa$B (NF-$\kappa$B) [91], another transcription factor that regulates aspects of innate and adaptive immune functions [92]. Which specific ROR1 functions that are mediated by crosstalk with these pathways is, however, not yet fully understood.

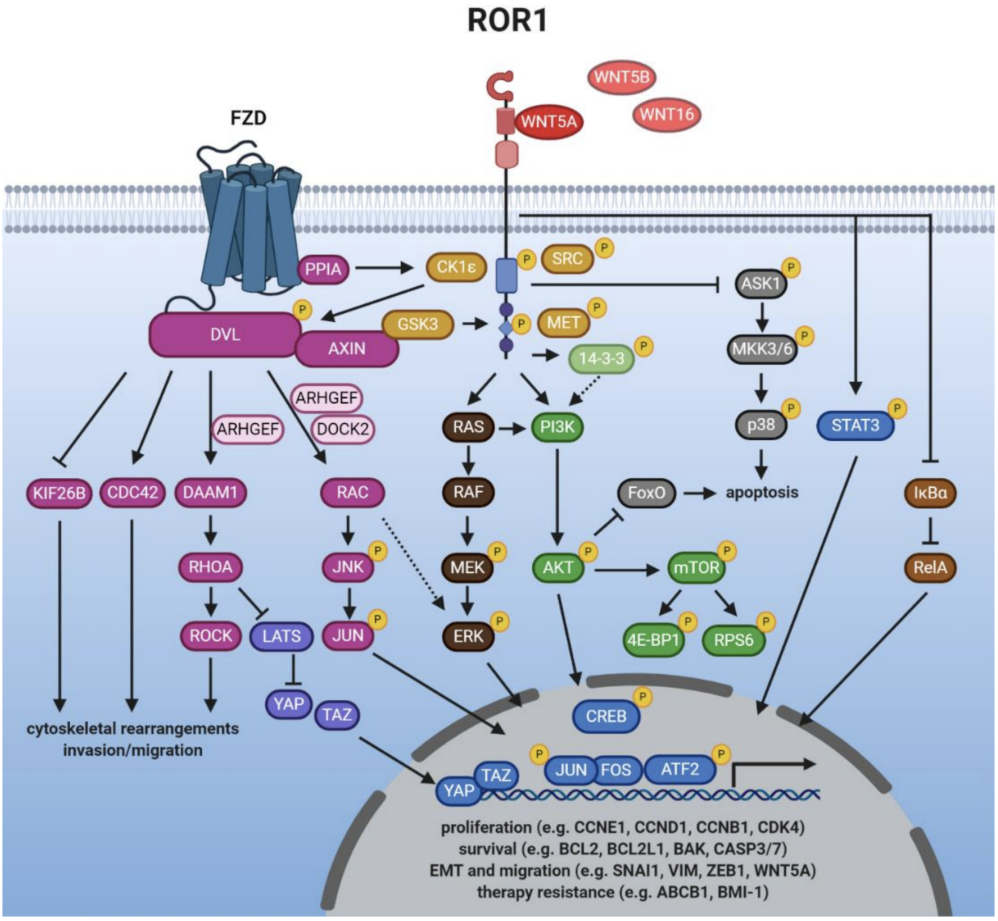


Figure 10: ROR1 signaling. Wnt/ROR signaling is induced by binding of a non-canonical Wnt ligand, which inititates the formation of a complex between ROR1 and ROR2, or ROR1 and a FZD receptor. Phosphorylation of ROR1 is mediated by several kinases (orange). This results in both the inhibition of anti-apoptotic pathways (grey) and the activation of of downstream pathways such as Wnt/PCP (magenta), MAPK/ERK (dark brown), PI3K/AKT (green), or NF-$\kappa$B (light brown). These pathways either trigger rearrangements of the cytoskeleton associated with increased tumor cell migration, or induce transcription of genes in the nucleus (blue) which leads to cell proliferation, survival, epithelial-to-mesenchymal-transition (EMT) and migration, or therapy resistance. Figure from [22].

### 2.8.3 Expression of ROR1 in cancer

Many studies have shown that ROR1 is highly expressed in malignant cells. Zhang et al. found expression of ROR1 in large proportions of many types of human cancers, including ovarian cancers, colon cancers, lung cancers, lymphomas, skin cancers, pancreatic cancers, testicular cancers, bladder cancers, uterus cancers, prostate cancers, and adrenal cancers [24]. However, ROR1 is not uniformly expressed in all cancer tissues, and its function may differ in the different cancer types [22]. Expression of ROR1 has been studied in hematological malignancies, particularly in chronic lymphocytic leukemia (CLL). The ROR1 gene was found to be 19-fold overexpressed in CLL compared to normal B cells [93]. Expression of ROR1 was also seen to increase with disease progression in CLL [94], and patients with high expression of ROR1 had significantly shorter therapy-free survival and overall survival, which indicates that ROR1 is associated with a more aggressive disease [95]. Furthermore, ROR1 expression has been demonstrated in many types of solid tumors. In colorectal cancer, ROR1 expression was seen to increase with clinical stage and lymph node metastasis, and can function as an indicator of disease progression [96]. Likewise, in ovarian cancer ROR1 expression was associated with tumor grade and lymph node metastases [97]. Particularly high levels of ROR1 expression was found in triple-negative breast cancer, the most aggressive breast cancer subtype, where very high expression was associated with shorter overall survival [84]. Breast cancer brain metastasis also showed high ROR1 expression, indicating that ROR1 plays a role in metastatic spread [98]. In lung cancer, ROR1 expression was seen to be particularly high in lung adenocarcinoma, where it can be used as an independent prognostic predictor for overall survival [99]. Moreover, high levels of ROR1 have been reported in prostate cancer. Zhang et al. found ROR1 expression in 19 of 21 (90%) of tested prostate cancers [24], while Sigvanesh et al. observed heightened ROR1 expression in the highly metastatic prostate cancer cell line PC3m, indicating that this protein may contribute to a more aggressive cancer [86].

### 2.8.4 Function of ROR1 in cancer

The increased expression of ROR1 in malignancies is mainly linked to its involvement in the non-canonical $\beta$-catenin-independent Wnt signaling pathway. Wnt signaling has been implicated as one of the main pathways in cancer development [23], and studies have associated overactive Wnt/ROR1 signaling with key tumorogenic processes such as cell survival, proliferation, and invasiveness [22]. The high expression of ROR1 in cancer cells may make this protein a target for anti-cancer therapies, and obtaining a better understanding of the functions of this protein in cancer has therefore gained increasing interest in cancer research.

A large number of studies have shown that ROR1 plays a major role in cancer cell survival, while at the same time counteracting apoptosis. This has been seen both in a variety of in vitro cancer cell line studies [100, 24, 101] and in xenograft studies in vivo [84, 102]. In a mouse model for human CLL, ROR1 expression accelerated the development of leukemia through interaction of ROR1 with the T cell leukemia 1 (TCL1) oncogene. This caused leukemia cell proliferation and resistance to apoptosis through pro-survival signaling via activation of the protein kinase AKT [103]. Silencing of ROR1 in lung cancer cells was shown to suppress the expression of important cell cycle regulators, while also increasing the expression of pro-apoptotic factors [104]. Recently, the pro-survival function of ROR1 has been suggested to be related to two new mechanisms; increase in activity of p53, a tumor suppressor gene, during ROR1 inhibition [87], and involvement of ROR1 in autophagy [104]. Further studies are needed to understand the role of ROR1 in these processes [22]. In ovarian cancer, a double KD of ROR1 and ROR2 was needed to see a significant reduction in proliferation of tumor cells [105], supporting a reciprocal regulation of the two in some cancers. Furthermore, in addition to ROR1 promoting cell survival through pro-mitotic factors, recent studies have also implied that it may control cellular structures involved in pro-survival signaling, such as filopodia [106, 107], whilch are actine-rich cell membrane projections that function as antennae for cells to probe their environment. Moreover, Wnt/ROR signaling has been established to increase resistance of cancer cells to chemotherapy and targeted therapy. Several studies have found increased expression of ROR1 in chemoresistant cancer cell lines [87, 108] and in patient tissues after chemo- or targeted therapy [109, 110]. In acute lymphoblastic leukemia (ALL), the sensitivity to several small molecule inhibitors in clinical use today was increased during KD of

ROR1 [89]. ROR1 has also been associated with treatment-resistant stem cells [111], suggesting that it might be involve in therapy resistance and relapse [22].

After the observations of ROR1's involvement in disease progression and metastases, studies have been conducted to investigate the role of this protein in the underlying cellular processes [22]. In CLL, cancer cells expressing ROR1 were stimulated with the Wnt5a ligand, and observations showed increased cell migration and chemotaxis [112], which is the directed migration of cells in response to concentration gradients of extracellular signals [113]. In support of this, reduction of chemotaxis was found during ROR1 KD in breast cancer cells [85]. Furthermore, the increase in cancer cell migration and invasion due to ROR1 expression might not only result from Wnt/ROR signaling, but has also been linked to the induction of epithelial-to-mesenchymal-transition (EMT) [22], which is a process where cells lose their adhesive characteristics and become more motile, which drives tumor spreading [22]. In breast cancer, tumors with high ROR1 expression showed an increase in expression of genes related to EMT compared to tumors with low ROR1 expression [85].

The function of ROR1 as a PTK is still poorly understood, although accumulating evidence have demonstrated its intrinsic tyrosine kinase activity [21]. In prostate cancer, high levels of ROR1 have been reported [24], although the expression of ROR1 and its kinase activity is not directly comparable. The action of ROR1, and not only its presence, was however validated in prostate cancer through measurements of the phosphorylated state of the protein in the master thesis by Mathilde Lystad [20]. Few studies have examined the function of ROR1 in prostate cancer specifically. Sivaganesh et. al. studied the role of ROR1 in aggressive prostate cancer and found that knocking down ROR1 reduces the phosphorylation of AKT and GSK3$\beta$, which should lead to reduction in survival, migration, and cell cycle progression of the cancer cells [86]. However, further studies are needed to investigate the role of ROR1 in this common type of cancer.

### 2.8.5 ROR1 in hypoxic tumors

In addition to an increase in ROR1 expression in cancer cells in genereal, studies have found high ROR1 expression in hypoxic compared to normoxic cancer cells. In the study by Lystad, kinase activity profiling of ROR1 was performed in prostate cancer cell lines PC3 and 22Rv1 under normoxic and hypoxic conditions, and an increased ROR1 kinase activity under hypoxia was observed [20]. Furthermore, Isomura et al. investigated the role of ROR1 in human lung adenocarcinoma cell lines, and found that ROR1 kinase activity was required for regulation of HIF-1$\alpha$ expression under both normoxic and hypoxic conditions. Specifically, they found that ROR1 inhibition alone was sufficient to suppress HIF-1$\alpha$ expression in both conditions [25]. Ishikawa et al. examined the effect of HIF-1$\alpha$ KD on hypoxia-induced expression of ROR1 in glioblastoma cells, and found that suppressed expression of HIF-1$\alpha$ inhibited expression of ROR1. They further investigated the possible involvement of HIF-1$\alpha$ in the transcriptional regulation of ROR1 gene, and found binding of HIF-1$\alpha$ to upstream regions of the ROR1 gene, indicating that expression of ROR1 might be regulated transcriptionally by HIF-1$\alpha$ [114]. HIF-1$\alpha$ is an important regulator of tumor adaptation to hypoxia, through its effect on various aspects of cancer development, including growth, angiogenesis, and metastasis. ROR1 thus appears to be a promising molecular target for treatment of hypoxic tumors.

# 3 Materials and Methods

*In vitro* cell studies were performed with the human prostate cancer cell line 22Rv1. The cell line was kept at the Department of Physics (DoP) at the Norwegian University of Science and Technology (NTNU), Trondheim, Norway.

## 3.1 Growth and cultivation of 22Rv1 cells

The 22Rv1 cells were grown as monolayers in $75\,\mathrm{cm}^2$ (TC75) or $25\,\mathrm{cm}^2$ (TC25) tissue culture flasks, or in 6-well culture plates, and incubated in a Binder Incubator at the DoP. The cells were maintained with RPMI-1640 growth medium (Thermo Scientific) supplemented with penicillin and fetal bovine serum (FBS) (10%). Subcultivation of the cells was performed twice a week to maintain exponential growth, and the growth medium was changed once a week.

## 3.2 Creation of hypoxic conditions

To obtain hypoxic conditions, an air-sealed plastic container (Thermo Scientific) was used for incubation of the cells. An Anaerobic Indicator (Thermo Scientific) was placed inside the box for indication of the oxygen level in the container. The indicator showed a bright pink color under normoxic conditions (21% $pO_2$), and a white color under hypoxic conditions ($pO_2 < 1\%$). To generate anaerobic conditions, an AnaeroPack-Anaerobic Gas Generator 2.5 l (Thermo Scientific) was used. This is a gas-generating sachet that maintains $pO_2 < 1\%$. The setup for hypoxic incubation is shown in Figure 11, where two TC25 flasks are placed inside the container.

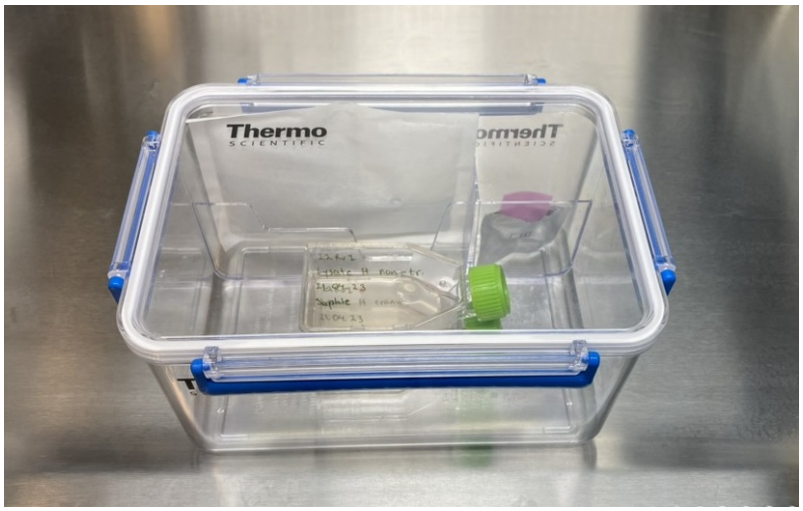


Figure 11: Hypoxic incubation of the cell culture flasks in an air-sealed plastic container, with an anaerobic atmosphere generator and an anaerobic indicator to monitor the oxygen level in the container.

The cells were incubated in the container as explained above for four hours prior to treatment, in order to equilibriate them in hypoxic conditions. The cells were incubated in the container for another four hours after treatment.

## 3.3 Knockdown of ROR1

KD of ROR1 was done in order to study cellular response to inhibition of ROR1. KD was done by transfection with the use of small interfering RNA (siRNA) and lipofectamine. siRNA functions

by interfering with expression of specific genes, preventing translation and the synthesis of proteins, in this case ROR1. Lipofectamine is a lipid based reagent, which increases the transfection effectiveness of siRNA. In order to exert the same strain on the cells where KD of ROR1 was not performed, negative control siRNA was used.

A protocol for KD of ROR1 by transfection was adapted from the Lipofectamine 2000 DNA Transfection Reagent Protocol (Invitrogen). The procedure is shown in Figure 12. Three days prior to transfection, 1 million cells were seeded in six TC25 flasks; three intended for ROR1 KD and three for control cells treated with negative control siRNA. Of these three TC25 flasks, two were used to make normoxic and hypoxic cell lysates and one was used to culture cells for the XTT cell viability and proliferation assay and the clonogenic survival assay.

At the day of transfection, 30 µl of Lipofectamine 2000 Reagent (1 mg/ml) (Invitrogen) was diluted in 1.5 ml of Opti-MEM I Reduced Serum Medium (Gibco), and incubated for 5 minutes in room temperature. To prepare the siRNA solution, 5 nmol of ROR1 Silencer Select Validated siRNA (Thermo Fisher) was diluted in 1.75 ml nuclease-free water, giving a siRNA concentration of 2.86 µM. A negative control siRNA solution was also prepared by diluting 5 nmol Silencer Select Negative Control siRNA (Thermo Fisher) in 1.75 ml of nuclease-free water. Then, 30 µl of the siRNA sample was further diluted in 750 µl Opti-MEM medium. 750 µl of this solution was transferred to a new tube, and mixed with 750 µl of Lipofectamine/Opti-MEM (1:1). The exact same procedure was performed for the diluted negative control sample. The solutions were gently mixed and incubated for 20 minutes at room temperature, to allow complex formation to occur. Next, 500 µl siRNA/Lipofectamine solution was added to each of the three ROR1-transfection TC25 flasks, and 500 µl negative control/Lipofectamine solution was added to the three control TC25 flasks. All flasks were rocked gently back and forth for mixing, and placed in incubation for three days before further analysis.

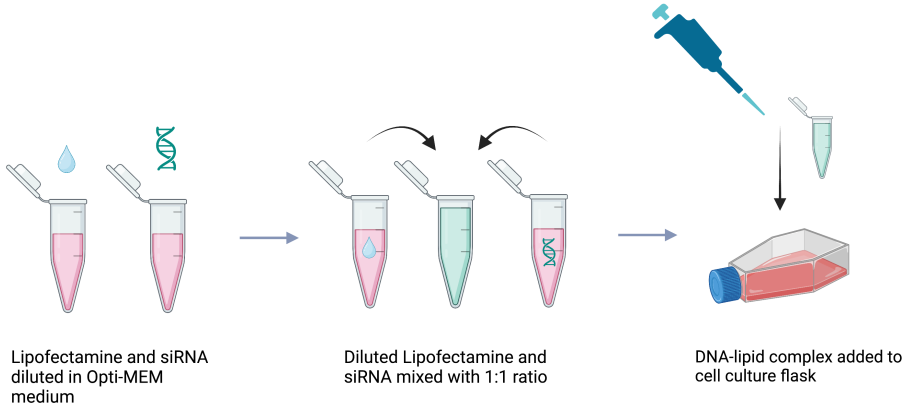


Figure 12: Procedure of ROR1 KD by transfection. Lipofectamine and siRNA was diluted in Opti-MEM medium, before the two solutions were mixed with a 1:1 radio. The siRNA-lipid complex was added to the cell culture flask. The cells were then incubated for 3 days before analysis. The exact same procedure was performed for the negative control siRNA.

## 3.4 Preparation of cell lysates

Cell lysates are preparations obtained from lysing cells by enzymatic, osmotic, or mechanical means. They can be obtaine from whole cells or from nuclear or cytoplasmic extracts. Lysing of whole cells cause the degradation or rupture of the cell membrane, the release of all cell contents, and the subsequent death of the cell [115]. It is used in laboratories to access and study the content of cells. In this study, whole cell lysates were used to examine expression of ROR1 in 22Rv1 cells with and without ROR1 KD under normoxic and hypoxic conditions.

Cell lysates were made from hypoxic and normoxic 22Rv1 cells three days after transfection. The preparation was performed by following a standard in-house protocol for cell lysates. As the purpose of lysate preparation was only to compare the expression of ROR1 in cells with ROR1 KD compared to those without ROR1 KD in hypoxic and normoxic conditions, no additional treatment was given to the cells. Only a placebo, 200 µl 10% DMSO in water, was added to each of the four TC25 flasks containing the cell samples; normoxic and hypoxic cells with ROR1 KD, and normoxic and hypoxic control cells. The hypoxic flasks were incubated in an anaerobic container for four hours prior to placebo addition, and for four hours immediately after placebo addition, as described in Section 3.2.

After incubation, lysates were prepared from the cell samples. A lysis buffer, used to disrupt the membrane of the cells, was prepared by mixing 980 µl of M-PER Mammalian Protein Exctraction Reagent (Thermo Scientific), 10 µl of Halt Protease Inhibitor Cocktail, EDTA-Free (Thermo Scientific), and 10 µl of Halt Phosphatase Inhibitor Cocktail (Thermo Scientific). The lysis buffer was put on ice. The growth medium was removed from the cell samples, which were then washed with 3 ml ice cold phosphate buffer saline (PBS) (Thermo Scientific). Then, 2 ml of ice cold PBS was added to each sample and the cells were scraped with an ice scraper in order to detach them from the bottom of the flask. The cell solution from each sample was transferred to an eppendorf tube, and centrifuged at 2500 rmp for 10 minutes at 4 °C. Next, the supernatant was removed, and 150 µl lysis buffer was added to each flask. The tubes were vortexed, incubated on ice for 30 minutes, and then centrifuged at 16 100 rpm for 15 minutes at 4 °C. Lastly, the supernatant was transferred to eppendorf tubes and stored at −20 °C until it was used for measurement of protein concentration in the samples and WB.

## 3.5 Measurement of protein concentration in cell lysates

Protein concentration was measured by the bicinchonic acid (BCA) assay. This method is based on the colorimetric detection and quantification of total protein in a sample. The method combines the reduction of $Cu^{2+}$ to $Cu^{1+}$ by protein in an alkaline medium, with the highly selective and sensitive colorimetric detection of $Cu^{1+}$ using a unique reagent containing BCA. The reaction product is purple in color and formed by chelation of two BCA molecules with one copper ion. This water-soluble complex exhibits a strong absorbance at 562 nm, which is nearly linear with protein concentration over a broad working range of 20-2000 µg/ml.

The BCA assay was performed according to the "Pierce BCA Protein Assay Kit" (Thermo Scientific). First, a BCA working reagent (WR) was prepared by adding 0.2 ml of BCA reagent B in 10 ml of BCA Reagent A (1:50). Then, 25 µl of pre-diluted standards consisting of 125-2000 µg/ml of the common protein bovine serum albumin (BSA) was added to a 96-well plate in triplicates, as shown in Figure 13. The same volume of the unknown samples was added to the plate in triplicates, in addition to a triplicate of a blank sample consisting of PBS. 200 µl of the WR was added to each well and the plate was incubated at 37°C for 30 minutes. After incubation, the plate was cooled to room temperature and the absorbance at wavelength 562 nm was measured with a SpectraMax i3x plate reader.

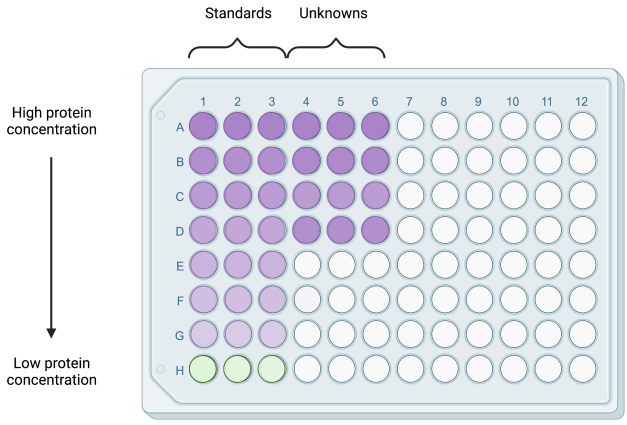


Figure 13: Illustration of the 96-well plate used in the measurement of protein concentration in cell lysates by the BCA assay. Triplicates were added of pre-diluted standards, unknown samples, and a blank samples consisting of PBS.

A standard curve was obtained based on the measured absorbance of the standard samples. The absorbance of the blank PBS samples was subtracted from all standard and unknown samples, and the average absorbance values for each standard and unknown sample was calculated from the triplicates. The standard curve was prepared in Excel, where the measured absorbance was plotted as a function of protein concentration. A linear regression fit was found, and the equation of this line was used to calculate the protein concentration of the unknown samples.

## 3.6 Western blotting with cell lysates

In order to detect and identify the ROR1 protein in cell lysates, Western Blotting (WB) was performed. WB was performed according to the "NuPAGE Bis-Tris Mini Gels" protocol (Invitrogen). The procedure consists of sample praparation, electrophoresis, transfer of gel to membrane, and immunodetection and imaging, as shown in Figure 14. WB of 22Rv1 ROR1 KD and control cells was performed with normoxic and hypoxic cell lysates.

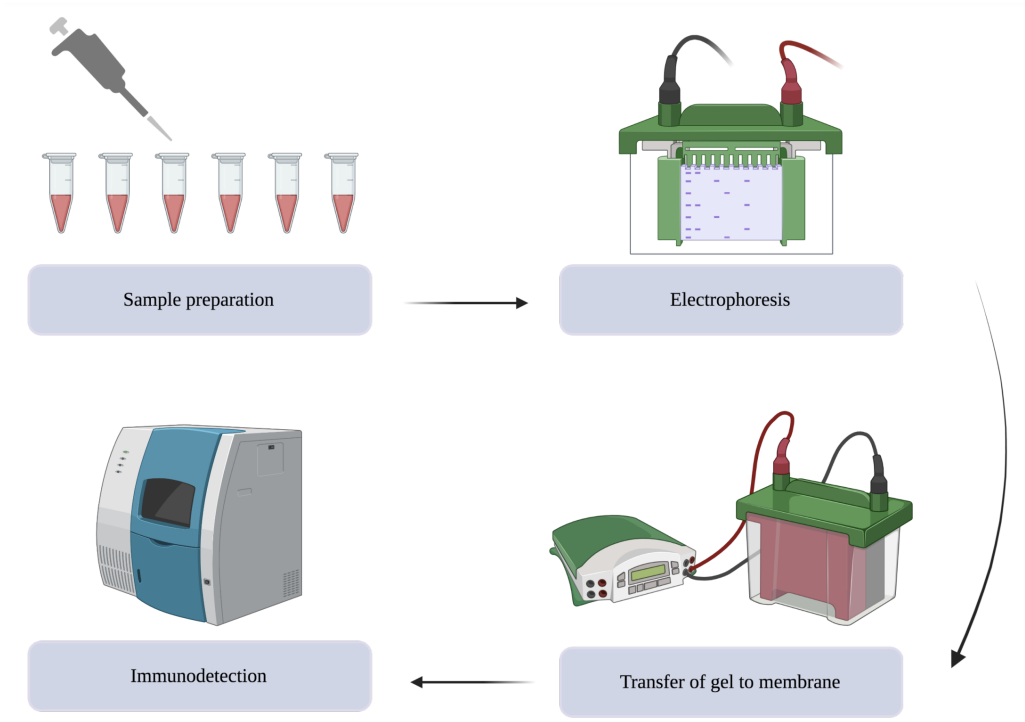


Figure 14: Workflow of western blotting with cell lysates. First, samples are prepared, then electrophoresis is performed, followed by transfer of gel to membrane, and lastly immunodetection takes place. Figure from [20].

**Sample preparation**: Protein in the samples was prepared for electrophoresis by denaturation and the addition of a negative charge. This is done so that the proteins migrate when subject to an electric field during electrophoresis.

The samples were prepared with 10 µg of protein. In order to obtain information about the protein concentration in each cell lysate, the BCA assay was performed for all samples prior to WB, see Section 3.6. The volume of cell lysates necessary for 10 µg of protein was mixed with 2.5 µl NuPAGE LDS Sample Buffer (x4) and 1 µl NuPAGE Reducing Agent (10x). De-ionized water was added to reach a total sample volume of 20 µl. The samples were heated in water at 70°C for 10 minutes.

**Electrophoresis**: Gel electrophoresis was performed in order to separate proteins based on molecular size. The proteins travel a distance in the gel that is determined by their molecular size, so that different bands represent proteins of different size. A band corresponding to the size of a specific protein can then be identified.

A running buffer was prepared by adding 50 ml NuPAGE SDS Running Buffer (x20) to 950 ml de-ionized water. A NuPAGE 10% Bis-Tris Gel, consisting of 10 wells, was prepared by rinsing the gel wells three times using the prepared running buffer. The gel was placed in an XCell Sure Lock Mini-Cell gel chamber (Invitrogen). As the chamber can be used with two gels at a time, a plastic Buffer Dam was placed in one of the gel slits. The chamber was then filled with running buffer so that the buffer level exceeded the level of the wells. Two wells in the gel were loaded with 5 µl of standards to obtain a protein ladder. The standards used were Precision Plus Protein Kaleidoscope (Bio-Rad) and MagicMark XP Western Standard (Invitrogen). 20 µl of each cell lysate sample was loaded in separate wells. The remaining wells were filled with 5 µl of LDS Sample Buffer (x4) to visualize the protein front. The gel was run at 100 V for 30 minutes, followed by 150 V for 15 minutes, and then 200 V for 15 minutes using a PowerEase Touch 120 W Power Supply (Invitrogen).

**Transfer of gel to membrane**: After electrophoresis was completed, the proteins had to be transferred from the gel to a solid membrane. This is done by the use of an electric field, which

pulls the proteins from the gel onto the membrane. The transfer is done in order to achieve a better handling capability and target protein accessibility for detection of the target protein.

A transfer buffer was prepared by mixing 50 ml of NuPAGE Transfer Buffer (20X) (Invitrogen) with 100 ml of 99.9% methanol (Sigma-Aldrich), and 850 ml of de-ionized water. After electrophoresis, the gel was removed from its cassette. For the transfer, an XCell II Blot Module (Invitrogen) was used. This is a wet-transfer module for the XCell SureLock systems that facilitates the transfer of proteins from gel to membrane. Four sponge pads for XCell II Blotting (Invitrogen) were soaked in the buffer, and two of them were placed in the cathode core of the blot module. A filter paper was placed on top of the sponges, followed by the gel, the transfer membrane, another filter paper, and the remaining two sponge pads. The transfer membrane used was a Nitrocellulose Membrane Filter Paper Sandwich (Invitrogen). The anode core was placed on top of the pads, closing the blot module. An illustration of the gel/membrane sandwich is shows in Figure 15. The blot module was positioned in the X Cell chamber and filled with transfer buffer until the gel/membrane sandwich was covered. The transfer was conducted at 30 V for one hour.

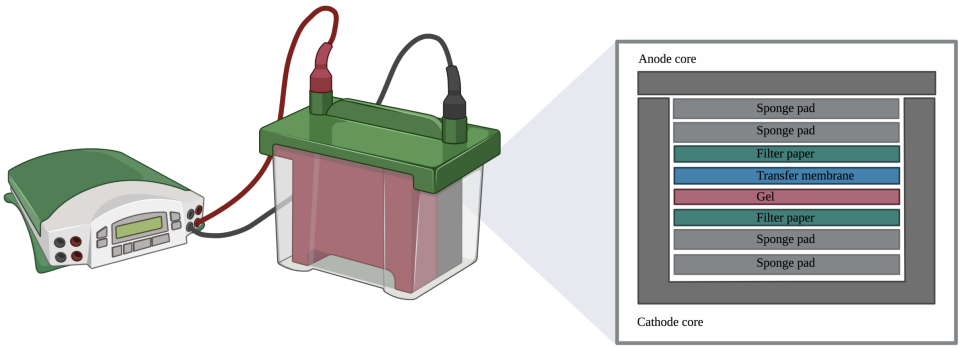


Figure 15: Transfer of gel to membrane, where 2 sponge pads were placed in the cathode core of the blot module, followed by a filter paper, the gel, the transfer membrane, another filter paper, and two more sponge pads. The anode core was placed in top of the pads, closing the blot module. Figure from [20].

**Immunodetection**: In order to detect and image specific proteins in the membrane, it must be incubated with the appropriate primary and secondary antibodies. The primary antibody is specific for the target protein, and is in turn recognized and bound by the secondary antibody, which is then conjugated with chemiluminescent molecules for detection. Before addition of antibodies, the membrane must be blocked to prevent unspecific binding.

The transfer membrane was removed from the gel/membrane sandwich and placed in a petri dish. A TBS-tween solution consisting of Tris Buffer Saline (1X) with 0.1% Tween 20 (Sigma-Aldrich) was used to rinse the membrane. The TBS-tween solution was made by dilution of TBS (10X) in de-ionized water. TBS (10X) was prepared by dissolving 24 g of Tris (Sigma-Aldrich) and 88 g of NaCl (Sigma-Aldrich) in 900 ml of DI water, and the pH of the solution was adjusted to $\sim$ 7.5 by addition of 12 M HCl (Sigma-Aldrich). Then, de-ionized water was added to the solution to reach a volume of 1 l, and 1 ml of Tween 20 was added. The membrane was rinsed once with TBS-tween, before blocking of the membrane was performed by addition of Starting Block Blocking Buffer (Thermi Scientific) until it covered the membrane. The membrane was then incubated with the blocking buffer for 30 minutes at room temperature with shaking on a plate shaker. The membrane was washed three times for ten minutes with TBS-tween at room temperature with shaking. A primary antibody solution was prepared by diluting 10 µl of a ROR1 Polyclonal Antibody (Invitrogen) in 10 ml TBS-tween. The membrane was incubated in the primary antibody solution with gentle agitation on a plate shaker overnight at 4°C. The washing process with TBS-tween was repeated. A secondary antibody solution was prepared by diluting 10 µl of HRP goat Anti-Rabbit IgG (Sigma-Aldrich) in 10 ml of TBS-tween. The membrane was incubated in this solution for one hour at room temperature with shaking, before the washing

process with TBS-tween was repeated.

To prepare the membrane for imaging, a chemiluminescent substrate consisiting of 1 ml of each of SuperSignal West Pico PLUS Stable Peroxide (Thermo Scientific) and SuperSignal West Pico PLUS Luminol/Enchancer (Thermo Scientific) was prepared. The substrate was added to the membrane, which was then incubated for 1 minute at room temperature. Next, the membrane was drained of excess chemiluminescent substrate and exposed by using a phosphor imaging device from Bio-Rad.

## 3.7 XTT cell viability and proliferation assay

XTT cell viability and proliferation assay can be used to measure cellular metabolic activity as an indicator of cell viability and proliferation. This assay is based on the reduction of a yellow tetrazolium salt to an orange formazan dye by metabolically active cells. The formazan dye that is formed is soluble in aqueous solutions and can be directly quantified by using a spectrophotometer. An increase in the number of living cells results in an increase in the overall activity of mitochondrial dehydrogenases in the sample. This increase directly correlates to the amount of orange formazan formed, and can be monitored by the absorbance. The XTT cell viability and proliferation assay was here used to compare the viability of 22Rv1 ROR1 KD cells and control cells under normoxic and hypoxic conditions.

The XTT assay was performed in accordance with the "XTT assay for Cell Viability and Proliferation" (Sigma Aldrich). A stock with a concentration of $10^6$ cells/ml was prepared from each of the ROR1 KD and control cells. Two 96-well plates were used for the assay, one for normoxic and one for hypoxic cells. In order to seed $4 \cdot 10^3$ cells in each well, the stock was diluted to a concentration of $4 \cdot 10^4$ cells/ml, before 100 µl of each diluted stock was added to 6 wells of the 96-well plate. Growth medium was also added to 6 wells of each plate for absorbance correction, as shown in Figure 16. The plates were then incubated for 12-24 hours.

On day two, in order to create hypoxic conditions, one of the plates was incubated in an anaerobic box for four hours, as described in Section 3.2. No additional treatment was given to the cells, but 10 µl of a placebo consisting of 10% DMSO in water was added to the cells and growth medium in order to exert the same physical strain on the cells that they would get from treatment. After placebo addition, the hypoxic cell plate was incubated in the anaerobic box for another four hours. Then, both plates were incubated under normoxic conditions for four days.

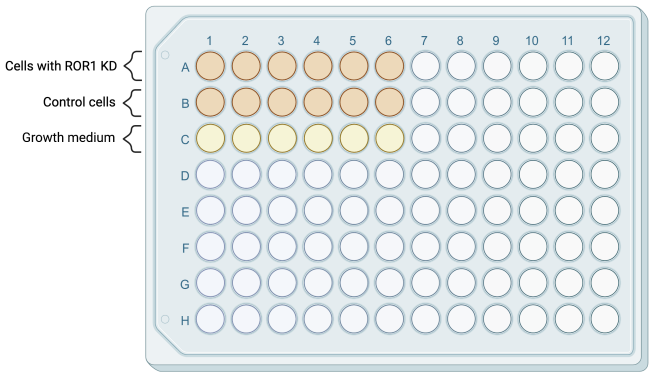


Figure 16: Illustration of the 96-well plates used for the XTT assay. Transfected cells, non-transfected cells, and growth medium was added in six wells each.

On day six, the XTT agent was added to the cells and the absorbance of the samples was measured. The XTT labeling mixture was prepared by addition of 40 µl Electron coupling reagent (Sigma-

Aldrich) to 2 ml XTT labeling reagent (Sigma-Aldrich). 50 µl of the XTT labeling mixture was added to each well in both plates, and the plates were incubated for four hours, with the hypoxic plate in the anaerobic box. The absorbance was measured at a wavelength of 575 nm with a SpectraMax i3x plate reader. The absorbance was also measured at 700 nm for reference.

## 3.8 Clonogenic survival assay

The clonogenic survival assay is a procedure used to assess whether a single cell has maintained its reproducibility after a given treatment. This is done by looking at the cells ability to form a colony, which is defined as 50 cells or more. By varying the amount of radiation or drug, a survival curve can be made, and the efficiency of the treatment can be assessed. In this study, the clonogenic survival assay was used to assess the viability of 22Rv1 cells with ROR1 KD compared to cells without ROR1 KD under normoxic and hypoxic conditions after exposure to varying amounts of ionizing radiation in the form of 2 MV photons.

An overview of the workflow of the clonogenic survival assay is shown in Figure 17. A stock was prepared from cultivated cells and used to seed a defined number of cells in 6-well petri dishes. After 12-24 hours, the cells were treated with varying doses of ionizing radiation. The cells were incubated for 14 days, before the colonies were fixed, stained, and counted. The assay was performed in three biological replicates with 22Rv1 cells. The mean survival of the three biological replicates was used to obtain a survival curve.

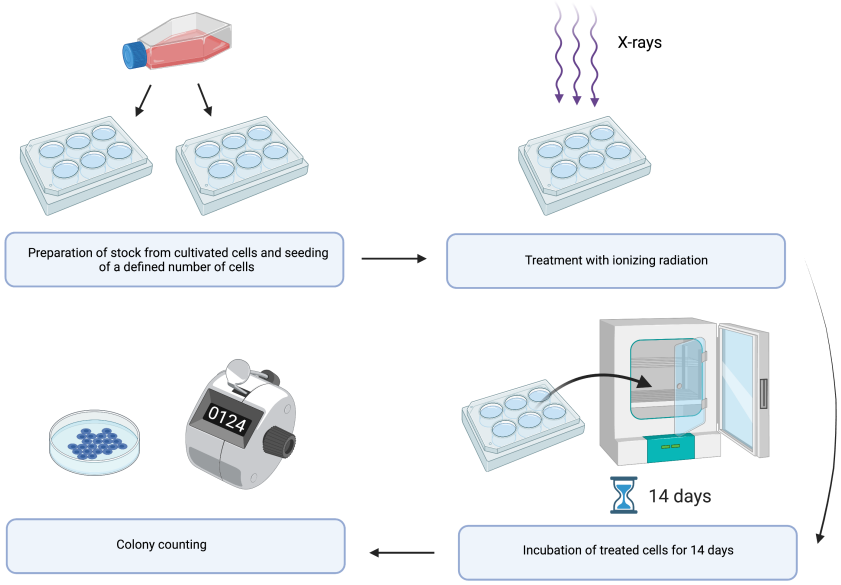


Figure 17: Illustration of the workflow of the clonogenic survival assay. A stock was prepared from cultivated cells, and a defined number of cells was seeded in 6-well plates. The cells were treated with ionizing radiation in the form of X-rays, before incubation for 14 days, and counting of the formed colonies.

The assay was performed following a standard in-house protocol. For each of the cultured cells with and without ROR1 KD, a stock of 1 million cells per ml was prepared. 20 µl of each stock was diluted in 1980 µl growth medium (1:100), obtaining new stocks of 10 000 cells/ml. Further dilutions were performed to prepare individual stocks for each irradiation dose to be used (0, 2, 4 and 6 Gy), where the concentration of cells per ml was increased with increasing irradiation dose, as shown in Table 1. The solutions were mixed well. The cells were seeded in eight 6-well plates, illustrated in Figure 18. Four plates were intended for hypoxia, and four for normoxia, with one hypoxic and normoxic plate receiving each irradiation dose. In each plate, 100 µl of cells with and without ROR1 KD were added in triplicates, together with 3 ml growth medium. The dishes were incubated for 12-24 hours, before irradiation with photons was performed using a linear accelerator

at St.Olavs hospital. The hypoxic cells were incubated in an anaerobic container for four hours prior to treatment, as described in Section 3.2. Irradiation was then performed, before the plates were immediately incubated in the anaerobic container for another four hours. Then, the cells were incubated for 14 days at 37°C under normoxic conditions.

Table 1: Dilutions of cell stock to be used for each dose of ionizing radiation in the clonogenic survival assay.

| **Dose [Gy]** | **Transfer from stock [µl]** | **Growth medium [µl]** | **Final concentration [cells/ml]** |
|---|---|---|---|
| 0 | 100 | 900 | 1000 |
| 2 | 200 | 800 | 2000 |
| 4 | 400 | 600 | 4000 |
| 6 | 800 | 200 | 8000 |

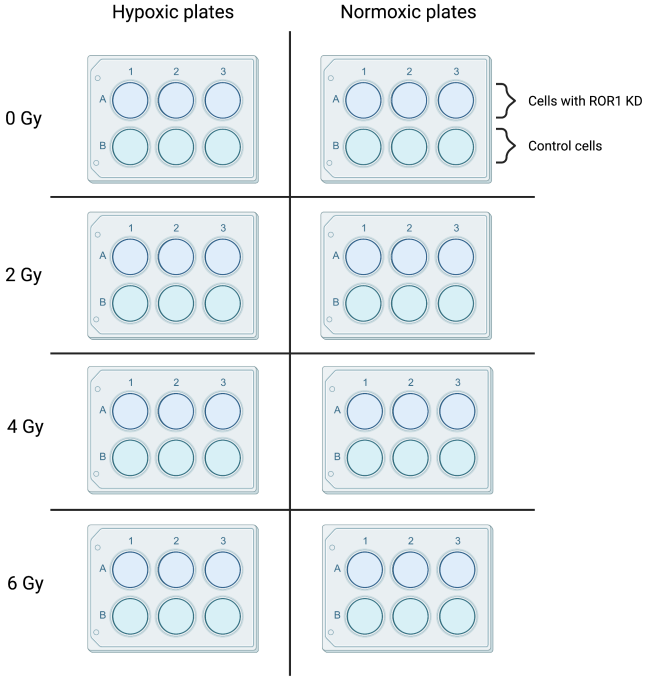


Figure 18: Overview of the eight 6-well plates used for the clonogenic survival assay for each replicate. Four plates were incubated in hypoxic conditions and four in normoxic conditions. For each of these, one plate was used for irradiation of 0, 2, 4 and 6 Gy, respectively. In each plate, cells with and without ROR1 KD were added in triplicates.

On day 14, the colonies were fixed and stained. The growth medium was removed for the wells, and 5 ml of 70% ethanol was added. The dishes were left to dry for 15 minutes at room temperature, before the ethanol was removed and 3 ml of a crystal violet solution was added. This solution was prepared by mixing 5 g of crystal violet (Sigma-Aldrich) in 500 ml 100% ethanol. The dishes were again left to dry for 30 minutes at room temperature. The crystal violet solution was removed from the dishes, before they were carefully rinsed with water and left to dry. Finally, the colonies in each dish were counted.

Survival curves were obtained from the average number of colonies counted for each irradiation dose in the three replicates. In order to calculate the percentage of survival after treatment, the plating efficiency (PE) must be taken into account. The PE value indicates the percentage of seeded cells that grow into colonies, and should ideally be 100% for untreated cells. However, due to factors such as suboptimal growth medium, errors, and uncertainties in counting the cell suspension, the PE is usually lower than 100% [45]. For each dose, the PE in percentage is given as

$$\mathrm{PE} = \frac{\text{average number of colonies counted}}{\text{number of cells seeded}} \cdot 100. \tag{6}$$

The percentage of survival at each dose of ionizing radiation is therefore given by

$$\text{Survival} = \frac{\text{average number of colonies counted}}{\text{number of cells seeded} \cdot \mathrm{PE(control)}/100} \cdot 100 = \frac{\mathrm{PE}}{\mathrm{PE(control)}} \cdot 100, \tag{7}$$

where PE(control) is the PE of the normoxic cells without ROR1 KD receiving 0 Gy of ionizing radiation.

# 4 Results

## 4.1 Protein concentration in cell lysates

The BCA protein assay was performed with all cell lysates in order to determine the protein concentration in each lysate. Based on the mean absorbance values of the standards, a standard curve was prepared. The standard curve displayed absorbance as a function of protein concentration, and is shown in Figure 19. From this, the protein concentration in each of the prepared 22Rv1 lysates was found, and these values are listed in Table 2.

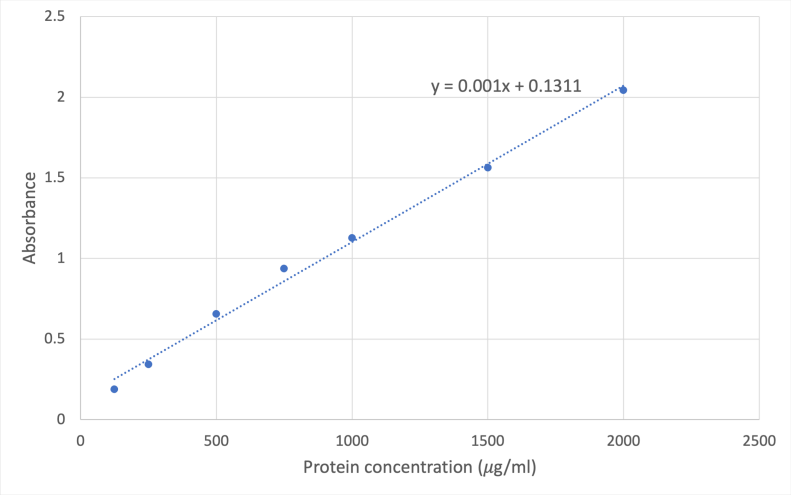


Figure 19: Standard curve of absorption as a function of protein concentration, prepared from the absorbance values of standards with known protein concentration in the BCA protein assay.

Table 2: Protein concentrations in lysates of 22Rv1 cells as found by the BCA protein assay.

| **Condition** | **Treatment** | **Protein concentration (µg/ml)** |
|---|---|---|
| Normoxic | None | 2220 |
| Hypoxic | None | 2147 |
| Normoxic | ROR1 KD | 2138 |
| Hypoxic | ROR1 KD | 2115 |

The resulting 96-well plate used for the BCA protein assay is shown in Figure 20. Columns 1-3 contain the standards used to obtain a standard curve for absorbance as a function of protein concentration. Columns 4-6 contain the samples with unknown protein concentration.

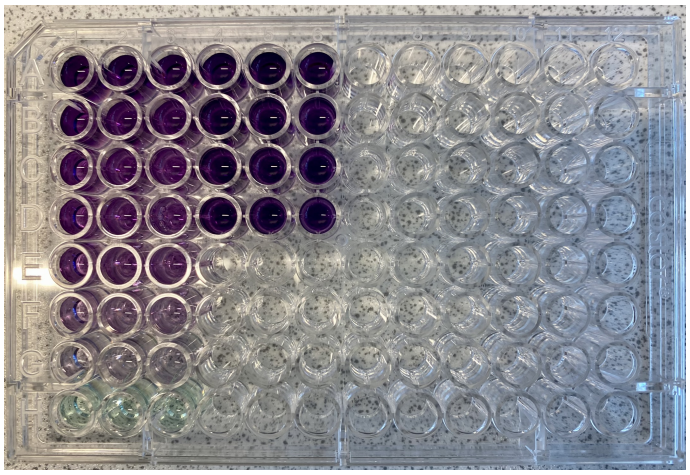

Figure 20: Resulting 96-well plate for the BCA protein assay. Columns 1-3 contain the protein standards ranging from high protein concentrations (top row) to low protein concentrations (bottom row) which were used to prepare a standard curve. Columns 4-6 contains lysates with unknown protein concentration.

## 4.2 Western blotting with cell lysates

WB was performed with an antibody against ROR1 in normoxic and hypoxic 22Rv1 cell lysates with and without ROR1 KD, in order to confirm ROR1 KD. Three attempts were made at confirming ROR1 KD by WB, which results are shown in Figures 21a, b, and c. Due to technical difficulties, none of the attempts were successful in validating ROR1 KD.

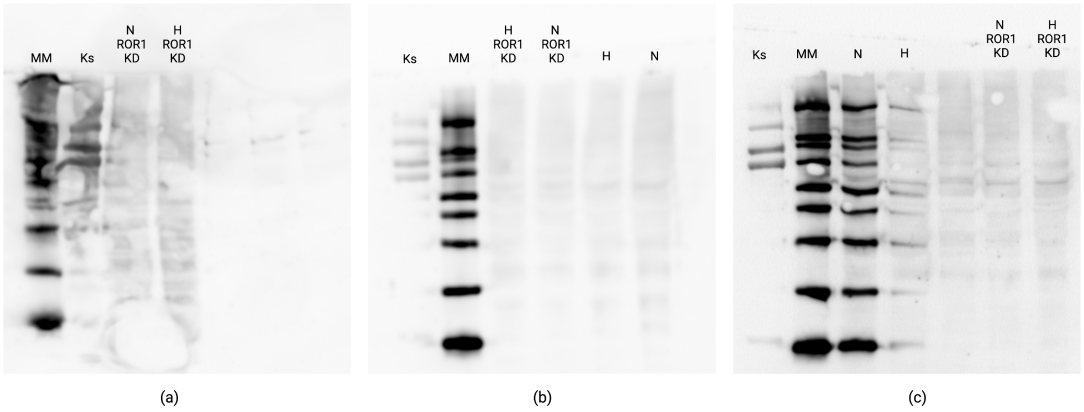


Figure 21: Resulting images of the membrane from the three attempts at WB for validation of ROR1 KD. The different columns represent samples containing the normoxic control (N), hypoxic control (H), normoxic ROR1 KD (N ROR1 KD) and hypoxic ROR1 KD (H ROR1 KD) cell lysate samples, in addition to the two standards Precision Plus Protein Kaleidoscope (Ks) and MagicMark XP Western Standard (MM).

Figure 21a represents the first attempt of validating ROR1 KD with WB. The resulting bands appear distorted and are not suitable for analysis of protein expression.

For the second attempt at WB for validating ROR1 KD, other filter papers were used and removal of air bubbles from the blotting pads before transfer of gel to membrane was improved. This resulted in a membrane with distinct columns for the different samples, as can be seen in Figure 21b. However, no clear protein bands appear in the columns. The molecular weight of ROR1 is

approximately 130 kDa, corresponding to the range between the first and second band from the top of the MagicMark (MM) standard. A successful validation of ROR1 KD would include a protein band in this range in the normoxic (N) and hypoxic (H) control samples, but not in the normoxic and hypoxic samples with ROR1 KD (N ROR1 KD and H ROR1 KD, respectively). The absence of such bands indicate that also this attempt was unsuccessful.

The third and final attempt at WB is shown in Figure 21c. In this attempt, new solutions of both the primary and secondary antibody were prepared with the aim of enhancing the binding of the antibodies to the membrane. Examining the N and H columns of the image, it appears as if some of the MM sample has leaked into these columns, as they contain protein bands corresponding to all reference bands in the MM column. Additionally, no protein bands corresponding to the molecular weight of ROR1 are observed in the N and H samples, deeming also this attempt unsuccessful. The ROR1 KD normoxic and hypoxic samples do not appear to be affected by leaking of MM. However, these bands cannot be used to assess the KD of ROR1 alone, as only the absence of a protein band at the molecular weight of ROR1 in the KD samples combined with the presence of a ROR1 protein band in the control samples would verify KD.

## 4.3 XTT cell viability and proliferation assay

The XTT cell viability and proliferation assay was performed with 22Rv1 cells in order to assess and compare the viability/metabolic activity of cells with and without ROR1 KD under normoxic and hypoxic conditions. The relative absorbance of the cells, as an indicator of cell viability, normalized to the normoxic control, is shown in Figure 22. The four bars in the figure represent the normoxic control (N Control), normoxic cells with ROR1 KD, hypoxic control (H Control) and hypoxic cells with ROR1 KD (H ROR1 KD). The hypoxic control showed an approximately 40% higher viability than the normoxic control. Additionally, cells with ROR1 KD showed a lower viability than control cells under both normoxic and hypoxic conditions, with a 9% decrease in metabolic activity of normoxic cells with ROR1 KD comapred to the normoxic control, and a 31% decrease in metabolic activity of hypoxic cells with ROR1 KD compared to the hypoxic control.

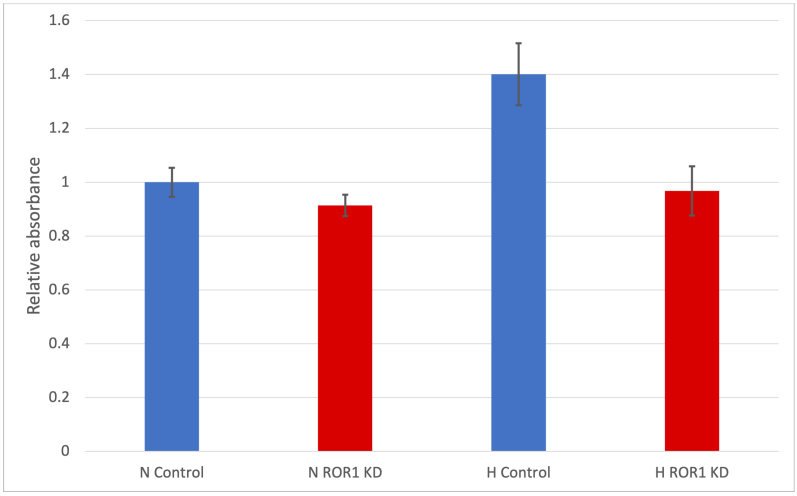


Figure 22: Relative absorbance of the four 22Rv1 cell samples; normoxic control (N Control), normoxic cells with ROR1 KD (N ROR1 KD), hypoxic control (H Control), and hypoxic cells with ROR1 KD (H ROR1 KD). All values are normalized to the absorbance of the normoxic control. Absorbance is presented as mean±SD (N = 3).

## 4.4 Clonogenic survival assay

The clonogenic survival assay was performed with normoxic and hypoxic 22Rv1 cells with and without ROR1 KD, in order to assess the cell survival of the cells after treatment with varying doses of ionizing radiation.

Survival in the different cell samples after irradiation is summarized in Table 3 and graphically represented in Figure 23, which indicate that treatment with ionizing radiation lead to a dose-dependent decrease in cell survival for all cell samples. The survival for each sample was normalized to the survival of the cells receiving 0 Gy of ionizing radiation. The highest cell survival was observed in cells without ROR1 KD incubated under hypoxic conditions (H Control) for all doses of ionizing radiation, where irradiation with 6 Gy resulted in 4.0% survival. For the same dose, normoxic cells without ROR1 KD (N Control) showed a 2.8% survival, corresponding to a 32% decrease compared to the hypoxic control. Cells with ROR1 KD displayed the lowest survival, with 2.0% for normoxic (N ROR1 KD) and 2.3% for hypoxic (H ROR1 KD) cells. This corresponds to a 28% decrease in survival for the normoxic cells with ROR1 KD compared to the normoxic control, and a 43% decrease in survival for the hypoxic cells with ROR1 KD compared to the hypoxic control.

Table 3: Survival in percentage of the cell samples receiving varying doses of ionizing radiation in the clonogenic survival assay. For each sample type (N Control, N ROR1 KD, H Control and H ROR1 KD), all values are normalized to the survival of cells receiving 0 Gy.

| **Dose (Gy)** | **Survival (%)** | | | |
|---|---|---|---|---|
| | N Control | N ROR1 KD | H Control | H ROR1 KD |
| 0 | 100.0 | 100.0 | 100.0 | 100.0 |
| 2 | 44.0 | 41.6 | 51.8 | 35.2 |
| 4 | 14.2 | 12.1 | 18.9 | 10.6 |
| 6 | 2.8 | 2.0 | 4.0 | 2.3 |

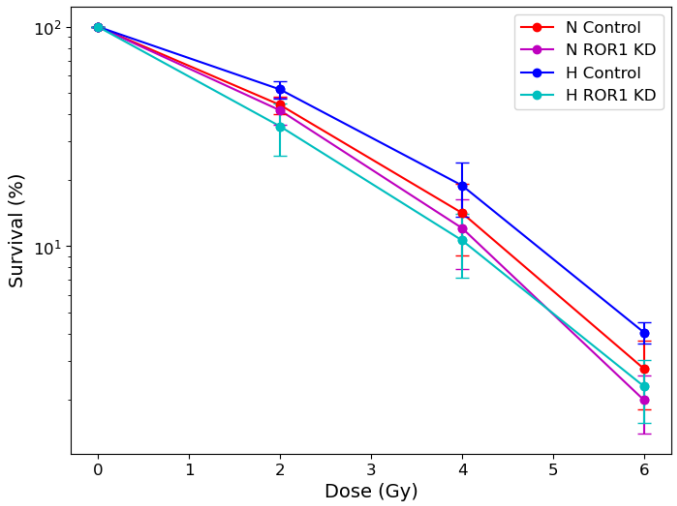


Figure 23: Survival of 22Rv1 cells with and withouth ROR1 KD in hypoxic and normoxic after treatment with varying doses of ionizing radiaiton. The hypoxic control (H control) showed the highest cell survival, followed by the normoxic control (H Control). Cells with ROR1 KD showed the lowest survival, where hypoxic ROR1 KD cell (H ROR1 KD) showed the lowest survival at 2 and 4 Gy, while normoxic ROR1 KD cells (N ROR1 KD) showed the lowest survival at 6 Gy. Survival is presented as mean±SD (N = 3) on a logarithmic scale in order to better visualize low survival rates.

An illustration of the resulting colony formation in one of the 6-well plates used in the clonogenic survival assay is presented in Figure 24, which shows the colonies of hypoxic cells receiving a dose of 2 Gy. The top row represents colonies of cells with ROR1 KD and the bottom row shows colonies of the control cells.

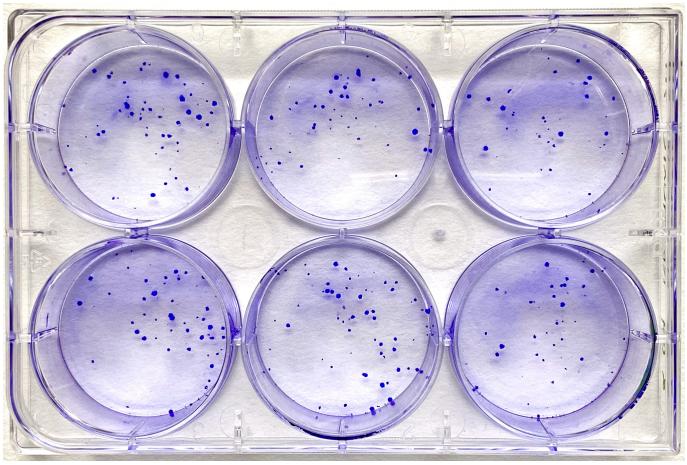

Figure 24: Illustration of the resulting colony formation after treatment with 2 Gy of ionizing radiation on hypoxic cells with ROR1 KD (top row) and control cells (bottom row).

# 5 Discussion

This project aimed to investigate the *in vitro* effects of ROR1 KD in the human prostate cancer cell line 22Rv1, on viability and survival after irradiation under normoxic and hypoxic conditions. Hypoxic tumors often show increased aggressiveness and resistance to treatment compared to normoxic tumors. The overexpression of ROR1 in various types of cancer has been demonstrated, and high ROR1 expression levels have been observed in hypoxic compared to normoxic cancer cells. As expression of ROR1 and cancer cell adaption to hypoxia seems to be interconnected, ROR1 arises as a possible target for TRT in hypoxic tumors. Additionally, the theranostic agent $^{64}$Cu-ES has previously shown great therapeutic effects in hypoxic prostate cancer cells, and a significant decrease in ROR1 expression has been observed after treatment with $^{64}$Cu-ES [20]. This study aimed to investigate if reduced activity of ROR1 may be responsible for the increased therapeutic effects of $^{64}$Cu-ES, and hence if ROR1 aids cancer cell survival.

KD of ROR1 was performed by transfection, and cell lysates were prepared from cells with and without ROR1 KD incubated under normoxic and hypoxic conditions. WB with cell lysates was performed with an antibody against ROR1 in order to validate ROR1 KD in the cells. Furthermore, the metabolic activity of the cells was examined by the XTT cell viability and proliferation assay, and the clonogenic survival assay was used to assess cell survival after treatment with different doses of ionizing radiation.

## 5.1 Creation of hypoxic conditions in the cells

Hypoxic conditions were created using an anaerobic container, as described in Section 3.2. This was an air-sealed plastic container with an anaerobic atmosphere generating sachet. An anaerobic indicator was placed inside the container for indication of the oxygen level, which showed a bright pink color when $pO_2 > 1\%$ and a white color when $pO_2 < 1\%$. This method was used for creation of hypoxic conditions in all *in vitro* cells studies in this project. It was desired to induce hypoxia in the cells in order to examine the effects of incubation in hypoxic compared to normoxic conditions on cell viability and survival. In particular, the effects of ROR1 KD in hypoxic compared to normoxic cells were of interest. It is therefore necessary to assess whether the method for creating hypoxic conditions in the cells was satisfactory for the purpose of this study.

The induction of hypoxic conditions inside the container was verified by the anaerobic indicator, which was observed to obtained a white color after approximately 30 minutes of incubation in all experiments in this study. However, it is another question whether hypoxia was in fact induced in the cells incubated in the container. Lystad, who conducted *in vitro* cell studies on 22Rv1 and PC3 cells under hypoxic and normoxic conditions, utilized the same method for creating hypoxic conditions in the cells [20]. To confirm induction of hypoxia in the cells, the expression of HIF-1$\alpha$ in cells incubated under hypoxia and normoxia was compared by performing WB with a HIF-1$\alpha$ antibody. It was observed that HIF-1$\alpha$ was expressed in cells incubated under hypoxic conditions, and not in cells incubated under normoxic conditions, and hence that hypoxia was induced in the cells by use of the anaerobic container system. No such confirmation of hypoxia induction was performed in this study. However, it is reasonable to assume that hypoxia was in fact induced in the cells also here, as the same cell line and exact same methods were used.

Additionally, Lystad found that the incubation of cells in hypoxic conditions for four hours prior to treatment and four hours after seemed to make the cells 30-40% less viable, and that this may imply that the oxygen level in the container was lower than the $pO_2$ of 0.1-1% commonly used to obtain hypoxic conditions in *in vitro* cell studies, but closer to anoxic conditions of $pO_2 < 0.1\%$ [20]. Interestingly, untreated cells incubated in hypoxic conditions in this study did not show decreased viability. Contrarily, the XTT cell viability and proliferation assay indicated higher viability for untreated cells incubated in hypoxic compared to normoxic conditions. It is therefore likely that the oxygen concentrations in this study was within the common range of 0.1-1%. Hublitz et al. used similar methods to create hypoxic conditions *in vitro* [116]. They reviewed the use of an oxygen absorber to generate hypoxic conditions in the dendrittic cell line JAWS II by the use of an air sealed container, and inferred that the oxygen level in the container was reduced to 0.2-0.3%.

This supports the claim that the oxygen levels in our study was in fact within the common working range for hypoxic conditions.

A variety of methods can be used to induce hypoxia *in vitro*. Cobalt chloride ($CoCl_2$) is a method where chemically induced pseudo-hypoxia is achieved, and HIF-1$\alpha$ is upregulated to mimic hypoxic conditions without actually adjusting the oxygen level [117]. This is a cost effective methode, however, the lack of actual changes in the oxygen concentration cause significant limitations [118]. Gas-controlled incubators, glove boxes, and acrylic incubator chambers are other methods that utilize nitrogen gas to achieve hypoxia, and usually allow for the control and monitoring of oxygen levels. However, nitrogen-based strategies are expensive. Nascimento-Filho et al. presented a cost-effective alternative to culturing cells under hypoxic conditions [117]. This method controlled the precise oxygen concentration with an oxygen absorber containing active powdered ion oxide, which was placed inside a self-sealed plastic bag containing the cell culture dishes. Four cell lines were used, including two head and neck squamous cell carcinomas (HNSCC) (WSU-HN12 and WSU-HN13), one human immortalized skin cell line (HaCaT), and one adenoid cystic carcinoma cell line from the salivary glands (UM-HACC-2A). The oxygen level in the container could be monitored continuously through the use of an oxygen meter placed inside the bag. Once the desired $pO_2$ level was achived, a second seal was placed in the bag to isolate the cells. The cells were incubated in hypoxic conditions for 1, 2, 6 and 24 hours after achieving oxygen levels of 2%. It was concluded that the use of this technique facilitated the desired hypoxic effects and allowed for the modification of the rate and duration of oxygen depletion in rapid-onset versus gradual-onset hypoxia, and acute versus chronic hypoxia, respectively. This method is similar to the one used in our study, as it involves an air sealed container and an oxygen absorbing pouch. However, it also allows for monitoring the exact oxygen level in the container and stabilizing the $pO_2$ at the desired level by sealing off the cells from the oxygen absorbing pouch.

Furthermore, another possibility for hypoxic incubation is to perform a cyclic evolution of the oxygen concentration. Along with chronic and acute hypoxic regions, solid tumors contain regions of cyclic variation of oxygen concentrations. These fluctuations occur due to changes in red blood cell flux, vascular remodelling and thermoregulationis [119], and are known as cyclic hypoxia or intermittent hypoxia. The changes in oxygen concentrations in cancer cells during cyclic hypoxia altes their susceptibility to treatment. Cyclic hypoxia is associated with increased cancer progression compared to acute and chronic hypoxia, involving enhancement in various hallmarks of cancer, including angiogenesis, immune evasion, metastasis, and survival [120]. The effects of cyclic hypoxia cannot be studied with static hypoxia models, such as the anaerobic container model used in this study. In order to get a better understanding of cancer cell response to ROR1 KD in hypoxic conditions inside real tumors, it would therefore be beneficial to use a model that accounts for the fluctuations of oxygen concentrations in the tumor. To do so one could induce cyclic hypoxia in the cell by periodic exposure to hypoxia and reoxygenation. This would require a method for creating hypoxic conditions that could monitor and control the exact level of oxygen in the environment of the cells at all times, and therefore a hypoxic workstation would be beneficial.

It can be argued that the method used for inducing hypoxia in the cells in this study worked for its purpose, as the actual induction of hypoxia in cells by incubation in the anaerobic container was validated by Lystad [20]. Although other methods, such as nitrogen-based workstations, may provide more stable $pO_2$ levels, $pO_2$ monitoring, and the possibility to study the effects of cyclic hypoxia in the cells, these methods would entail a significant investment and cost increase. The method by Nascimento-Filho et al. [117] does, however, show potential for a less expensive technique that also allows for more precise $pO_2$ level monitoring and stabilization. This method could be considered for future studies.

## 5.2 Methods of ROR1 knockdown

ROR1 KD was performed in order to assess the *in vitro* effects of ROR1 on viability and survival of the prostate cancer cell line 22Rv1. In this section, the method for achieving ROR1 KD will be discussed.

ROR1 KD was performed by transfection, which is a process by which foreign nucleic acids are

delivered into a cell in order to modify the host cell's genetic content. This was done by the use of siRNA, which functions by inducing gene-specific RNA degradation in the cells, enabling the specific knockdown of genes. siRNA was combined with lipofectamine, which is a common transfection reagent that is used to increase the transfection efficiency of RNA. This method has been validated in a number of *in vitro* cell studies. Liu et al. performed ROR1 KD in lung adenocarcinoma cells by transfection using siRNA [121]. ROR1 expression was examined by flow cytometry 72 hours after transfection, and a decrease in ROR1 expression of 50-90% was observed. The same method was used by Henry et al., who studied ROR1 KD in ovarian cancer, and observed a significant decrease in ROR1 expression after transfection [108]. Although KD by transfection is a well-established method, which is used in most studies performing ROR1 KD, it does only cause temporary KD of the gene of interest, and maximal effect, first achieved on day 2-3 post-transfection, only last for 5-7 days [122]. This method does therefore not reflect the long-term effects of ROR1-blocking in cancer cells. This may have affected cell survival in the clonogenic survival assay in our study, as colony counting was done up to 15 days after maximal effect of transfection was assumed to occur. Although it is considered most critical obtain ROR1 KD in the cells at the time of irradiation, subsiding of ROR1 KD during incubation while awaiting colony formation may have affected the proliferation of the cells in this time and hence the results of the assay.

In addition to transfection by siRNA, several other methods exist to perform KD of specific proteins, including the use of short hairpin RNA (shRNA). This approach uses a small piece of RNA that is converted by cells to siRNA, which can in turn induce gene-specific RNA degradation. shRNA is useful because it can be delivered to cells by viral vectors, which allows for control of the expression of the shRNA with inducible promoters and simultaneous delivery of other genes [123]. Additionally, studies examining the effects of transfected siRNAs and plasmids expressing shRNAs indicate that shRNAs are superior with respect to duration and efficiency of gene knockdown [123]. shRNA enables the establishment of stable KD cell lines, i.e. cell lines where the KD of specific proteins is permanent. Stable ROR1 KD was performed in a lung adenocarcinoma cell line by Zhou et al., by injection with lentiviruses containing shRNA with a specific human ROR1 targeting sequence [104]. ROR1 KD was verified by flow cytometry with inhibition rates of 35-55%, depending on the cell type. To our knowledge, no studies performing ROR1 KD by the use of shRNA in prostate cancer cell lines exist. However, this method may provide better conditions for assessing the long term effects of ROR KD in 22Rv1 cells *in vitro*, and may have been better suited for ROR1 KD prior to the clonogenic survival assay in this study.

## 5.3 Validation of ROR1 knockdown

In order to confirm ROR1 KD, WB was performed with normoxic and hypoxic cell lysates, using an antibody against ROR1. Due to technical difficulties, WB was performed in three replicates, where none resulted in successful validation of ROR1 KD.

The first replicate of WB (Figure 21a) showed distorted columns in the membrane, and it was concluded that this resulted from use of the wrong filter papers and insufficient removal of air bubbles from the blotting pads during the transfer of gel to membrane. This assumption was based on observations during the procedure, as the column of the Kaleidoscope standard (Ks), which is visible in the gel and on the membrane with the naked eye, was straight with defined bands when observed in the gel. However, after the transfer of gel to membrane, the structure of the column and bands had changed.

The missteps made in the first WB replicate were corrected in the second replicate (Figure 21b), which resulted in an overall improved structure of the columns in membrane. This membrane showed no signs of air bubble distortion and had well defined protein bands of the Magic Mark (MM) standard. However, no protein bands were observed corresponding to the molecular weight of ROR1, which was expected for the normoxic and hypoxic samples without ROR1 KD. As high levels of ROR1 expression has been shown in prostate cancer [84, 86], the absence of ROR1 expression in the 22Rv1 cells in this study is unlikely, and other possible reasons for the missing bands must be explored. As the overall structure of the columns on the membrane appeared as it should be, it was concluded that the electrophoresis and transfer of gel to membrane were likely

not the cause of the absent bands. It was therefore hypothesized that an error had occurred either in the preparation of the samples, or during the labelling of the membrane with antibodies. New solutions of both the primary and secondary antibody were prepared and the same membrane was incubated once more with the new antibody solutions. However, this caused no change in the resulting images.

For the third replicate (Figure 21c), the membrane was again incubated in new solutions of the antibodies, in an attempt to detect ROR1 bands. Additionally, to ensure that the protein content in the samples was high enough for detection, the volume of lysate added to the samples before gel electrophoresis was doubled. This replicate was, however, influenced by what appears to be mixing of the samples in the different wells, causing the bands of the MM to appear in the samples of the normoxic control (N) and hypoxic control (H). As ROR1 KD would only be verified by the presence a band corresponding to the molecular weight of ROR1 in the normoxic and hypoxic control columns and the absence of one in the normoxic ROR1 KD (N ROR1 KD) and hypoxic ROR1 KD (H ROR1 KD) columns, the disturbance caused by MM bands in the samples deemed also this attempt unsuccessful. The mixing of the samples was most likely due to insertion of the pipette tip too deep into the well during the loading of the samples onto the gel, causing the gel and wells to move when the pipette was extracted. Moreover, the mixing of the samples made it difficult to determine whether the doubling of the protein content in the samples had an effect on the ROR1 bands.

Even though the procedure for WB is simple, many problems can arise that lead to unexpected results. In this study, the main issue was the absence of a protein band corresponding to the molecular weight of ROR1. The absence of bands can arise due to a variety of reasons associated with antibody, antigen, or buffer used. One possibility for the unsuccessful WBs is poor quality of the antibodies used. As the ROR1 primary antibody was newly purchased, this antibody should be well functioning. However, the secondary antibody had been stored in-house for an unknown period of time. Secondary antibodies last for up to two years when frozen, and this time may be shortened by exposing the antibody to many freeze/thaw cycles. It is therefore possible that the secondary antibody had decayed over time and did not label the membrane properly. To check the binding of the secondary antibody, incubation and immunodetection of the membrane with only the secondary antibody could be performed. The appearance of the MM band indicates that at least one of the antibodies worked for their purpose, as MM contains nine recombinant binding sites (20-220 kDa), each of which contains a binding sites for either the primary or secondary antibody.

Additionally, the lack of recorded signal may be related to the concentration of antibody, where a low concentration could cause a weak signal. However, the protocol used for performing WB in this study was a standard in-house protocol, which had been used several times previously with successful outcome. It is therefore unlikely that the concentration of antibody was too low. Moreover, the signal can be decreased by prolonged washing, and the washing buffer used can contribute to the problem. The washing buffer used in this study was newly prepared according to a standard protocol for the preparation of TBS-tween, and should therefore not cause problems related to aging of the buffer. However, there is always a possibility of the buffer being contaminated. For examples, contamination of buffers with sodium azide can inactivate HRP, which is the detection label conjugated to the secondary antibody used in WB [124].

Other possible reasons for low signal in WB are related to low concentrations of protein in the lysate samples, or insufficient exposure time during immunodetection. Regarding the concentration of protein in the samples, it is necessary to have a sufficient amount of protein for detection of signal. According to the in-house WB protocol, 10 µg of protein was needed for each sample. The volume of lysate necessary to satisfy this was calculated from the protein concentration of each samples, as determined by the BCA assay. The samples should therefore have contained enough protein to obtain a successful WB. Still, the protein content was doubled in the third replicate in this study, although the effects of this were inconclusive due to the mixing of samples. Furthermore, the exposure time during immunodetection was set to the maximum possible time, and is therefore also unlikely to have caused the absence of a ROR1 band. Additionally, the high intensity of the bands in the MM column suggests adequate exposure time.

In summary, there are many factors that may have contributed to the unsuccessful WB and validation of ROR1 KD. Assuming there were no errors in the gel electrophoresis and transfer of gel to membrane of the second replicate, the problem is likely related to the washing and labelling of the membrane with the secondary antibody. The use of a new secondary antibody for labelling of the membrane could potentially create a better result. However, due to time limitations, this was not done in this study.

Although the attempts at WB for validating ROR1 KD in this study were unsuccessful, the results from the XTT cell viability and proliferation assay and the clonogenic survival assay suggests that the KD of ROR1 itself was in fact successful. The XTT assay indicated a decrease in cell viability of the samples with attempted ROR1 KD for both normoxic and hypoxic conditions. Additionally, the result from the clonogenic survival assay showed a lower cell viability after irradiation with photons for the cells with attempted ROR1 KD. This is in accordance with the variety of studies that have indicated a correlation between expression of ROR1 and cancer cell survival [21, 100, 24, 101]. The results from these experiments will be further discussed in the following sections.

Other methods for validating ROR1 KD are also worth mentioning. A variety of studies have verified ROR1 KD with other methods, however, often in combination with WB. Henry et al. [108], who studied ROR1 KD in overian cancer, confirmed KD by quantitative real-time polymerase chain reaction (qRT–PCR). This is a method for quantifying the level of messenger RNA (mRNA), a type of single-stranded RNA involved in protein synthesis, in a sample, in addition to WB. This method has displayed high specificity, good reproducibility, and a wide dynamic range [125]. By performing qRT-PCR alone or in combination with WB, more reliable results regarding expression of the ROR1 gene and protein in our this study may have been obtained. Additionally, flow cytometry can be performed for analysis of relative expression levels of ROR1. This method utilizes fluorescently-tagged antibodies to identify cells expressing a protein or receptor of interest. Fluorescent detectors within the flow cytometer are used to determine the amount of fluorescence emitted by cells, which indicates level of protein expression [126]. The advantages of this method are that it enables multiplexed and quantitative analysis of signaling events with greater sensitivity and precision than WB, in just a few hours [127].

## 5.4 Cell viability following hypoxic incubation

The results of the XTT assay (Figure 22) indicated that the metabolic activity of the control cells incubated under hypoxic condtitions was approximately 40% higher than that of the cells incubated under normoxic conditions. This indicates that hypoxia itself did not decrease the viability of the cells, but instead increased it. Additionally, the observed change in viability of the cells after hypoxic incubation compared to normoxic incubation validates the induction of hypoxia in the cells.

There is a general consensus that hypoxic tumors are resistant to cancer treatments such as radiotherapy and chemotherapy. There is, however, more variability in the observed effects of hypoxia in untreated cells. Hypoxia has been shown to reduce cell proliferation in numerous cancer cell types [128]. Most studies also show decreased viability of prostate cancer cells in hypoxia compared to normoxia [129, 130]. However, hypoxia has also been observed to induce responses in cancer cells that lead to increased viability, such as altered gene expression and suppression of apoptosis [131]. The results from the XTT assay in our study indicate that 22Rv1 cells belong to the latter group. This is supported by a study by Rios-Colon et al., who studied the effect of KD of CPT1A, an important enzyme in metabolism of fat, in hypoxic and normoxic 22Rv1 cells [132]. They assessed cell viability by the use of the MTT assay, which is a colorimetric assay for measuring cell metabolic activity similar to the XTT. Their results indicated higher viability of untreated cells incubated under hypoxic compared to normoxic conditions. However, they did not provide any discussion on the reason for the increased viability in hypoxic cells, as this was not the main subject of their study. Nonetheless, their results support the increase in viability of 22Rv1 cells after incubation in hypoxia.

An increase in metabolic activity as seen by the XTT assay could either mean more cells in the sample or increased metabolic activity of the individual cells. Higgins et al. studied the metabolic

activity of three prostate cancer cell lines (LNCaP, DU145 and PC3) under hypoxia. They found that lactate production was increased and that ATP levels were decreased in all cell lines under hypoxic compared to normoxic conditions [133]. Under low oxygen conditions, when the demand for oxygen and ATP exceeds the cellular supply, the metabolism in cells is adapted to be able to supply the cell with energy. Glucose in the cytoplasm is then converted to pyruvate, which is directly reduced to lactate [134]. Increased lactate levels is therefore a sign of metabolic activity in hypoxic cells. Although we have not been able to find similar studies on 22Rv1 cells, the occurrence of increased metabolism in several other prostate cancer cell lines indicates that the increased metabolic activity measured in the XTT assay of in this study may be due to same effect; increase of metabolic activity in individual cells.

## 5.5 Effects of ROR1 knockdown on cell viability and survival

To assess the *in vitro* effects of ROR1 KD, the XTT and the clonogenic survival assay were performed. The former measures the metabolic activity of the cells, while the latter evaluates cell survival. The cells examined in the XTT assay received no other treatment than ROR1 KD and hypoxic incubation, while the cells in clonogenic survival assay were in addition treated with different doses of ionizing radiation by photons, in order to assess the dose-dependent survival of cells with ROR1 KD compared to control cells. For both methods, the effects of ROR1 KD in cells incubated in hypoxic compared to normoxic conditions were studied. In the following, the methology of the two methods, as well as the cellular response to ROR1 KD, will be discussed.

The XTT assay is based on the measurement of color changes in the growth medium. This measure is different for different types of medium, in addition to being influenced by air bubbles in the wells and the temperature during reading. Due to these effects, the clonogenic survival assay, which is the golden standard to measure cell survival, is often used instead. The XTT assay only shows a snapshot of the *in vitro* effects of ROR1 KD, while the clonogenic survival assay shows the effect on the cells over time, and hence give a better image of actual survival. The clonogenic survival assay does, however, not provide information on the type of cell death induced in the irradiated cells, as cell death can be caused by a variety of different methods, including apoptosis, necrosis, autophagy and senescence [135]. The XTT assay is more susceptible to variations in the number of cells seeded in the wells, especially since the cells with ROR1 KD and control were cultured in separate flasks. In the clonogenic survival assay, the number of colonies counted are normalized to the samples receiving 0 Gy of radiation, removing this uncertainty. A drawback of the clonogenic survival assay compared to XTT is the time consumption, as there is a 10-14 day waiting period to allow for the formation of colonies. However, in this study, the two assays were used to look at different effects of ROR1 KD. The XTT was used to look at the effects of ROR1 KD itself on cell viability, in hypoxic and normoxic cells, compared to control cells. The clonogenic survival assay was used to assess whether ROR1 KD has an effect on cell survival after irradiation. It would also be possible to use the clonogenic survival assay to examine the effect of ROR1 KD itself, by comparing the number of colonies formed of the cells receiving an irradiation dose of 0 Gy, although this method would also be affected by uncertainties in cell seeding.

When performing the clonogenic survival assay, the size of the resulting colonies of the 22Rv1 cells were varying in size. This is probably due to differences in the effect of irradiation on individual cells, were in some cases, irradiation decreased but not completely inhibited cell survival. Due to the differences in size of the colonies, the clonogenic survival assay relies on the subjective decision of whether a group of cells should be counted as a colony (50 or more daughter cells) or not. To obtain a reference, some colonies were investigated under a microscope in order to identify groups of cells with more than 50 cells. However, the colonies of the 22Rv1 cells were small in size, which made it challenging to distinguish between groups of cells with more and less than 50 daughter cells. To make the same subjective assessment of colony size, the colonies of the three replicates of the clonogenic survival assay was counted during the same week.

The results of the XTT assay (Figure 22) indicated a decrease in metabolic activity of prostate cancer cells with ROR1 KD compared to untreated cells, with a mean 31% decrease for hypoxic ROR1 KD cells compared to the hypoxic control, and mean 9% decrease in normoxic ROR1 KD cells compared to the normoxic control. As previously discussed, a mean 40% increase in metabolic

activity was observed in the hypoxic control compared to the normoxic control. However, after ROR1 KD, hypoxic cells showed a considerable decrease in metabolic activity, down to 3% less than the normoxic control. This suggests that the presence of ROR1 influenced cell viability, and that ROR1 KD reduced the viability of prostate cancer cells, especially under hypoxic conditions.

Few studies have examined the effect of ROR1 KD on cell viability in hypoxia. However, Isomura et al. studied the effects of ROR1 KD in mice and found the involvement of ROR1 in regulation of HIF-1$\alpha$ expression [25]. ROR1 KD was observed to strongly inhibit lung tumor development and growth, and ROR1 inhibition alone was shown to be sufficient to supress HIF-1$\alpha$ expression under both normoxic and hypoxic conditions. This study also used WB to examine expression of ROR1 and HIF-1$\alpha$ in normoxic and hypoxic cells. Since HIF-1$\alpha$ regulates many responses of tumor cells to hypoxia, the suppression of this transcription factor by ROR1 KD could contribute to the decreased viability of hypoxic prostate cancer cells observed in our study.

A similar method to the XTT assay for assessing the effects of ROR1 KD was used by Liu et al, who studied silencing of ROR1 by siRNA in human lung adenocarcinoma tissues and cell lines, and found that ROR1 silencing significantly down-regulated the activity of the PI3K/AKT/mTOR signaling pathway [121]. This is associated with significant apoptosis and anti-proliferation of tumor cells. To assess cell viability, they performed the MTS Cytotoxicity assay, which, similarly to the XTT assay, is based on the reduction of a tetrazolium compound by viable cells to generate a colored formazan dye that is soluble in cell culture medium [136]. All cell lines silenced for ROR1 showed reduced growth rates relative to a control. This supports our results of reduced cell viability after ROR1 KD.

Regarding prostate cancer, Sivaganesh et. al. studied the role of ROR1 in the prostate cancer cell lines LNCaP, PC3, and a highly metastatic variant of PC3, PC3m [86]. In order to assess the effects of ROR1 KD on downstream proteins, WB was performed with antibodies against ROR1, AKT and GSK3$\beta$. It was found that ROR1 KD reduced the phosphorylation of AKT and GSK3$\beta$, which should lead to reduction in survival, migration, and cell cycle progression of the cancer cells. Similar results were found in lung adenocarcinoma by Zhou et al., who studied stable silencing and long-term effects of ROR1 KD [104]. They found that ROR1 KD suppressed the expression of important cell cycle regulators, while also increasing the expression of pro-apoptotic factors. Their data indicated that ROR1 KD could deregulate activation of AKT and GSK3$\alpha/\beta$. They concluded that ROR1 KD could effectively regulate the cell cycle, apoptosis, and autophagy in lung cancer. This study used a human phospho-kinase array to examine relative levels of protein phosphorylation. As GSK3$\beta$ is a regulator of glycogen metabolism, this could have contributed to the decreased metabolic activity observed in 22Rv1 cells by the XTT assay in our study.

The results from the clonogenic survival assay (Figure 23) indicated that the hypoxic control had the highest cell survival after irradiation, for all irradiation doses. This is expected, as hypoxia is known to induce enhanced survival and lead to increased resistance of cancer cells to radiotherapy. The normoxic control showed decreased cell survival for all doses compare to the hypoxic control, with the largest reduction being 32% at 6 Gy. The increased survival of the hypoxic control compared to the normoxic control is in accordance with the oxygen effect, i.e. that oxygen deficiency in tissue causes decreased biological damage by ionizing radiation. However, the difference in survival between the normoxic and hypoxic control is less than the commonly seen OER of 2.5-3.5 for X-rays.

Interestingly, cells with ROR1 KD showed the lowest survival in the clonogenic survival assay. The greatest differences are again observed at the highest dose of 6 Gy, where a 28% and 43% decline was observed in the normoxic ROR1 KD cells compared to the normoxic control and the hypoxic ROR1 KD cells compared to the hypoxic control, respectively. The decrease in cell survival of the normoxic ROR1 KD cells compared to the normoxic control indicates that ROR1 must be present and active in normoxic cells. The results from the clonogenic survival assay are in line with the results from the XTT assay, were KD was seen to reduce the metabolic activity of the cells. The clonogenic survival assay also indicates that ROR1 KD reduces the radioresistance of the cells, especially under hypoxic conditions.

To our knowledge, no other studies have examined the survival of cancer cells following ROR1 KD and treatment with ionizing radiation by use of the clonogenic survival assay. However, in a study

by Ghaderi et al., colony formation of non-small cell lung cancer (NSCLC) after treatment with a small molecule ROR1 inhibitor (KAN0441571C) was examined. Their results indicated that the drug compromised the clonogenic survival of the cells and that an increased dose of the inhibiting molecule caused less colony formation [137]. This supports the result from the clonogenic survival assay in our study, indicating that a decrease in ROR1 activity causes decreased survival of cancer cells.

## 5.6 ROR1 and Cu-64-Elesclomol

This study was initiated by the findings of Lystad, who inferred that treatment with $^{64}$Cu-ES in the prostate cancer cells lines PC3 and 22Rv1 provided a great therapeutic effect [20]. Through kinase activity profiling, she also observed that this radiopharmaceutical decreased the kinase activity of ROR1. Based on these findings it was hypothesized that $^{64}$Cu-ES showed a significant effect in decreasing the survival of prostate cancer cells due to its ability to reduce ROR1 activity. High levels of ROR1 expression has previously been reported in prostate cancer [24, 86]. Our study indicates that ROR1 not only has a high expression in prostate cancer, but also must have a role in the viability and survival of prostate cancer cells, as both the XTT and clonogenic survival assay showed decreased survival of 22Rv1 cells after ROR1 KD. These findings strengthen the hypothesis that the therapeutic effect of $^{64}$Cu-ES may be linked to ROR1 activity.

Based on previous knowledge of the cellular mechanisms of Cu-64 and ES, as described in Section 2.6, the findings of Lystad [20], and the results obtained in this study regarding the effects of ROR1 KD on cell viability and survival, the superior therapeutic effect of $^{64}$Cu-ES may be explained by a combination of radiation-induced and chemical-induced cell death. This may be attributed to three main mechanisms; First of all, the ability of ES to transport copper into the mitochondria of cells may cause elevation of oxidative stress levels and subsequent induction of apoptosis. Secondly, trapping of Cu-64 in the mitochondria of the cells allow for AE delivery to the mitochondria, which has been argued to be more susceptible to ionizing radiation than the cell nucleus [19], and cause radiation-induced cell death. Finally, $^{64}$Cu-ES cause reduction in ROR1 activity in the cells, which in this study has been shown to lead to decreased cell survival, both alone and in combination with ionizing radiation. The reduced cell survival in prostate cancer cells with ROR1 KD after irradiation may indicate that the reduction in ROR1 activity caused by $^{64}$Cu-ES increases the susceptibility of the cancer cells to AE emission originating from the same compound. Additionally, as described in Section 2.8.2, ROR1 participates in cell signaling, especially as a co-receptor for the non-canonical Wnt signaling pathway, which has been associated with development of many types of cancer when unusually regulated. Furthermore, the apparent role of ROR1 as a crossroad that can link Wnt signals to other major signaling pathways involved in important cellular processes, such as PI3K/AKT, MAPK/ERK, and NF-$\kappa$B, may contribute to the therapeutic effects of decreased ROR1 activity by $^{64}$Cu-ES. The results of this study therefore supports a further investigation of the exact mechanisms of reduction in ROR1 activity by $^{64}$Cu-ES and downstream effects on the associated signaling pathways.

# 6 Further work

In further work, WB can be performed again, in order to properly validate ROR1 KD. Additionally, other methods for assessing the expression of ROR1 and its protein-encoding gene, such as flow cytometry and qRT-PCR may be used, either alone or in combination with WB, for more reliable results. Several studies have used qRT-PCR or flow cytometry in combination with WB to examine ROR1 protein and gene expression [138, 139, 140]. Zhou et al. even utilized all three methods to confirm establishment of cells with stable ROR1-silencing in lung adenocarcinoma [104].

Additionally, the anaerobic container used to create hypoxic conditions in the cells in this study could be replaced by an hypoxia workstation, or by the self-sealed plastic bag containing active powdered ion oxide introduced by Nascimento-Filho et al. [117], as both allow for better monitoring and control of the oxygen levels. By use of an hypoxic workstation it would also be possible to induce cyclic hypoxia in the cells, which may provide a better model for the oxygen conditions in real tumors.

In order to assess the long-term effects of ROR1 KD in cancer cells, a cell line with permanent ROR1 KD can be established by the use of shRNA, as was done by Zhou et al. [104]. They created ROR1-stably silenced clones from PC9, PC9erlo, and NCI-H1975 cell lines, and studied the long-term effects of ROR1 KD in lung adenocarcinoma. By obtaining cell lines with permanent ROR1 KD, *in vivo* experiments could be performed, where this cell line is injected into mice to see if these cells exchibit less growth than cells with functioning ROR1. Other methods for silencing of ROR1 could also be performed, such as the use of ROR1 inhibitors, as was done by Ghaderi et al., who studied clonogenic survival of NSCLC cells after treatment with a small molecule ROR1-inhibitor [137]. However, as inhibitors are often not completely specific, the creation of cell lines with permanent ROR1 KD is likely the best option.

Moreover, the effects of ROR1 KD on cell viability and survival could be examined in other cell lines, both in prostate cancer and other types of cancer. This study only examined ROR1 KD effects in one prostate cancer cell line. However, high ROR1 expression has been observed in a variety of human cancers [24], and other studies indicate that ROR1 affects viability and survival in other cancer cell types, such as CLL [112], breast cancer [85], and lung adenocarcinoma [104].

It could also be of interest to assess by which mechanism the cells die after ROR1 KD and/or treatment with $^{64}$Cu-ES. For example, flow cytometry can be utilized for simultaneous assessment of necrosis and apoptosis [141]. Additionally, autophagy can be measured by detection of the autophagy marker protein microtubule-associated proteins 1A/1B light chain 3B (LC3), through fluorescence microscopy, WB with antibodies against LC3, or flow cytometry [142].

Additionally, downstream signaling of ROR1 could be examined. Several studies have identified ROR1 as a co-receptor for Wnt signaling. Lystad found that ROR1 activity was decreased in hypoxic PC3 and 22Rv1 cells, compared to a normoxic control. In 22Rv1 cells she found that the activity of ROR1 and protein tyrosine kinase 7 (CCK4/PTK7) was strongly decreased after treatment with ES. Both are co-receptors for non-canonical Wnt signaling. This supports that there is an effect on this pathway after treatment. Further studies can be done to characterize how $^{64}$Cu-ES affects this pathway in detail.

As this study strengthened the hypothesis that the superior therapeutic effects of $^{64}$Cu-ES is linked to decreased activity of ROR1, further studies could also be focused on examining the exact mechanisms by which $^{64}$Cu-ES decreases ROR1 activity in prostate cancer cells.

Furthermore, in the continued development of theranostic radionuclides, translational research is important. This means that in addition to developing new theranostic radionuclides for clinical applications, thorough characterization of these agents in experimental models is needed. The process of translating results from the laboratory into real-world practice involves several steps, including pre-clinical and animal studies, and phase 1, 2, 3 and 4 clinical studies. In order for the discoveries to have the highest possible chance of success, it is important to understand the science and operational principles underlying each step of the translation process [143].

Theranostic radionuclides in cancer treatment represent major potential for future applications.

This field has grown in parallel with the advancements in molecular imaging and personalized medicine, and can help to provide customized treatment of various cancers in improving patient selection, prediction of response and toxicity, and determination of prognosis [8]. Buatti et al. reviewed the evolution of theranostic in radiation oncology, and summarized the advantages of this treatment over other molecular target therapies [144]. These included less treatment resistance and greater antitumor efficiency, the possibility of optimizing the dose for each patient by use of quantitative PET and SPECT to make complete voxel-wise dosimetry maps of a radiopharmaceutical, and lessened biological effects in healthy tissue by delivering a low dose rate over several days to weeks. However, there are still many practical and biological challenges that need to be addressed regarding this type of cancer treatment. Marin et al. argued that the biggest question is how to evaluate treatment response, and whether functional (CT and MRI) or anatomical (PET) imaging should be used to define progressive disease [8]. Nevertheless, current developments indicate that this type of personalized treatment will be available to patients in the future [145].

# 7 Conclusion

In this study, the response of the prostate cancer cell line 22Rv1 to ROR1 KD was investigated in hypoxic compared to normoxic conditions. For this purpose, ROR1 KD was performed in the cells by transfection. Cell lysates were prepared for WB with a ROR1 antibody, with the aim of validating ROR1 KD. Metabolic activity of the cells was investigated by the XTT cell viability and proliferation assay, and cell survival after irradiation with X-rays was assessed with the clonogenic survival assay. The results from these methods were analyzed and compared.

ROR1 KD was observed to reduce metabolic activity and cell survival of the human prostate cancer cell line 22Rv1, both in normoxic and hypoxic conditions. Cell survival was decreased in a dose-dependent manner after treatment with ionizing radiation by photons in both conditions. The greatest cellular response to ROR1 KD was seen in hypoxia, both in terms of metabolic activity and cell survival after irradiation.

This study indicates that there is a correlation between ROR1 activity and cancer cell viability and survival, and that this interaction is increased in hypoxia. The study supports further investigation of ROR1 mechanisms in cancer. Additionally, it strengthens the hypothesis that the increased therapeutic effect of $^{64}$Cu-ES is linked to decreased ROR1 activity. Further experiments should focus on uncovering the mechanisms by which $^{64}$Cu-ES inhibits ROR1, in addition to mechanisms of ROR1 activity itself, including its downstream signaling. Effects of ROR1 KD in other cell lines could also be examined, and cells with permanent ROR1 KD could be established in order to examine the long-term effects of ROR1 KD.

# References


[1] Hyuna Sung et al. 'Global cancer statistics 2020: GLOBOCAN estimates of incidence and mortality worldwide for 36 cancers in 185 countries'. In: *CA: a cancer journal for clinicians* 71.3 (2021), pp. 209–249. DOI: 10.3322/caac.21660.

[2] Cancer Research UK. *Cancer survival statistics*. URL: https://www.cancerresearchuk.org/%20health-professional/cancer-statistics/survival#heading-Zero (visited on 20th Apr. 2023).

[3] Roghayyeh Baghban et al. 'Tumor microenvironment complexity and therapeutic implications at a glance'. In: *Cell Communication and Signaling* 18 (2020), pp. 1–19. DOI: 10.1186/s12964-020-0530-4.

[4] Asieh Emami Nejad et al. 'The role of hypoxia in the tumor microenvironment and development of cancer stem cell: a novel approach to developing treatment'. In: *Cancer Cell International* 21.1 (2021), pp. 1–26. DOI: 10.1186/s12935-020-01719-5.

[5] Bill Harris et al. 'Targeting hypoxia in solid and haematological malignancies'. In: *Journal of Experimental & Clinical Cancer Research* 41.1 (2022), p. 318. DOI: 10.1186/s13046-022-02522-y.

[6] Joseph C Walsh et al. 'The clinical importance of assessing tumor hypoxia: relationship of tumor hypoxia to prognosis and therapeutic opportunities'. In: *Antioxidants & redox signaling* 21.10 (2014), pp. 1516–1554. DOI: 10.1089/ars.2013.5378.

[7] Xinming Jing et al. 'Role of hypoxia in cancer therapy by regulating the tumor microenvironment'. In: *Molecular cancer* 18 (2019), pp. 1–15. DOI: 10.1186/s12943-019-1089-9.

[8] José Flávio Gomes Marin et al. 'Theranostics in nuclear medicine: Emerging and re-emerging integrated imaging and therapies in the era of precision oncology'. In: *Radiographics* 40.6 (2020), pp. 1715–1740. DOI: 10.1148/rg.2020200021.

[9] Tengzhi Liu et al. 'Hypoxia imaging and theranostic potential of [64Cu][Cu (ATSM)] and ionic Cu (II) salts: a review of current evidence and discussion of the retention mechanisms'. In: *EJNMMI research* 10.1 (2020), pp. 1–14. DOI: 10.1186/s13550-020-00621-5.

[10] Ute Maucksch et al. 'Radiotoxicity of alpha particles versus high and low energy electrons in hypoxic cancer cells'. In: *Nuklearmedizin-NuclearMedicine* 57.02 (2018), pp. 56–63. DOI: 10.3413/Nukmed-0950-17-12.

[11] Atsushi Obata et al. 'Basic characterization of 64Cu-ATSM as a radiotherapy agent'. In: *Nuclear medicine and biology* 32.1 (2005), pp. 21–28. DOI: 10.1016/j.nucmedbio.2004.08.012.

[12] Jason S Lewis et al. 'Copper-64-diacetyl-bis (N 4-methylthiosemicarbazone): an agent for radiotherapy'. In: *Proceedings of the National Academy of Sciences* 98.3 (2001), pp. 1206–1211. DOI: 10.1073/pnas.98.3.1206.

[13] Paul Burgman et al. 'Cell line-dependent differences in uptake and retention of the hypoxia-selective nuclear imaging agent Cu-ATSM'. In: *Nuclear medicine and biology* 32.6 (2005), pp. 623–630. DOI: 10.1016/j.nucmedbio.2005.05.003.

[14] Amy L Vāvere and Jason S Lewis. 'Examining the relationship between Cu-ATSM hypoxia selectivity and fatty acid synthase expression in human prostate cancer cell lines'. In: *Nuclear medicine and biology* 35.3 (2008), pp. 273–279. DOI: 10.1016/j.nucmedbio.2007.11.012.

[15] Peijie Zheng et al. 'Elesclomol: a copper ionophore targeting mitochondrial metabolism for cancer therapy'. In: *Journal of Experimental & Clinical Cancer Research* 41.1 (2022), pp. 1–13. DOI: 10.1186/s13046-022-02485-0.

[16] Paolo Ettore Porporato et al. 'Mitochondrial metabolism and cancer'. In: *Cell research* 28.3 (2018), pp. 265–280. DOI: 10.3390/ijms21093363.

[17] Poorva Ghosh et al. 'Mitochondria targeting as an effective strategy for cancer therapy'. In: *International journal of molecular sciences* 21.9 (2020), p. 3363. DOI: 10.1038/cr.2017.155.

[18] Masazumi Nagai et al. 'The oncology drug elesclomol selectively transports copper to the mitochondria to induce oxidative stress in cancer cells'. In: *Free Radical Biology and Medicine* 52.10 (2012), pp. 2142–2150. DOI: 10.1016/j.freeradbiomed.2012.03.017.

[19] Winnie Wai-Ying Kam and Richard B Banati. 'Effects of ionizing radiation on mitochondria'. In: *Free Radical Biology and Medicine* 65 (2013), pp. 607–619. DOI: 10.1016/j.freeradbiomed.2013.07.024.

[20] M. H. Lystad. *In vitro studies of Cu-64 radiopharmaceuticals for targeted radionuclide therapy of hypoxic tumors*. [Master thesis, NTNU]. 2022.

[21] Yuming Zhao et al. 'Tyrosine kinase ROR1 as a target for anti-cancer therapies'. In: *Frontiers in Oncology* 11 (2021), p. 680834. DOI: 10.3389/fonc.2021.680834.

[22] Kerstin Menck et al. 'The WNT/ROR pathway in cancer: from signaling to therapeutic intervention'. In: *Cells* 10.1 (2021), p. 142. DOI: 10.3390/cells10010142.

[23] Virginia Murillo-Garzón and Robert Kypta. 'WNT signalling in prostate cancer'. In: *Nature Reviews Urology* 14.11 (2017), pp. 683–696. DOI: 10.1038/nrurol.2017.144.

[24] Suping Zhang et al. 'The onco-embryonic antigen ROR1 is expressed by a variety of human cancers'. In: *The American journal of pathology* 181.6 (2012), pp. 1903–1910. DOI: 10.1016/j.ajpath.2012.08.024.

[25] Hisanori Isomura et al. 'Conditional Ror1 knockout reveals crucial involvement in lung adenocarcinoma development and identifies novel HIF-1$\alpha$ regulator'. In: *Cancer science* 112.4 (2021), pp. 1614–1623. DOI: 10.1111/cas.14825.

[26] National Institutes of Health (US). *Biological Sciences Curriculum Study. NIH Curriculum Supplement Series*. National Institutes of Health (US), 2007. Chap. Understanding Cancer.

[27] Eric J Hall and Amato J Giaccia. *Radiobiology for the Radiologist*. 7th ed. Lippincott Williams & Wilkins, 2012. Chap. 18. Cancer Biology, pp. 273–302.

[28] Douglas Hanahan and Robert A Weinberg. 'Hallmarks of cancer: the next generation'. In: *cell* 144.5 (2011), pp. 646–674. DOI: 10.1016/j.cell.2011.02.013.

[29] Chris Sumner. *Hallmarks of Cancer: Activation Invasion and Metastasis*. URL: https://blog.cellsignal.com/hallmarks-of-cancer-activation-invasion-and-metastasis (visited on 25th Apr. 2023).

[30] D. Ribatti. 'Angiogenesis'. In: (2013). Ed. by Stanley Maloy and Kelly Hughes, pp. 130–132. DOI: https://doi.org/10.1016/B978-0-12-374984-0.00065-6.

[31] National Cancer Institute. *Radiopharmaceuticals: Radiation Therapy Enters the Molecular Age*. URL: https://www.cancer.gov/news-events/cancer-currents-blog/2020/radiopharmaceuticals-cancer-radiation-therapy (visited on 25th Apr. 2023).

[32] Kenneth S Krane. *Introductory nuclear physics*. John Wiley & Sons, 1991.

[33] Kenneth S Krane. *Introductory nuclear physics*. Second edition. John Wiley & Sons, 1991. Chap. 6. Radioactive decay, pp. 160–191.

[34] Kenneth S Krane. *Introductory nuclear physics*. Second edition. John Wiley & Sons, 1991. Chap. 8. Alpha decay, pp. 246–271.

[35] Kenneth S Krane. *Introductory nuclear physics*. Second edition. John Wiley & Sons, 1991. Chap. 9. Beta decay, pp. 272–326.

[36] Anthony Ku et al. 'Auger electrons for cancer therapy–a review'. In: *EJNMMI radiopharmacy and chemistry* 4.1 (2019), pp. 1–36. DOI: 10.1186/s41181-019-0075-2.

[37] Nasrin Abbasi Gharibkandi et al. 'Nanostructures as radionuclide carriers in auger electron therapy'. In: *Materials* 15.3 (2022), p. 1143. DOI: 10.3390/ma15031143.

[38] Jason P Holland et al. 'Copper-64 radiopharmaceuticals for oncologic imaging'. In: *PET clinics* 4.1 (2009), pp. 49–67. DOI: 10.1016/j.cpet.2009.04.013.

[39] S. Nord. *Dosimetric evaluation of MR-only treatment planning for photon and proton therapy in prostate cancer*. Specialization project in Applied Physics and Mathematics, NTNU. 2022.

[40] Eric J Hall and Amato J Giaccia. *Radiobiology for the Radiologist*. 7th ed. Lippincott Williams & Wilkins, 2012. Chap. 1. Physics and Chemistry of Radiation Absorption, pp. 3–11.

[41] V. Lobo et al. 'Free radicals, antioxidants and functional foods: Impact on human health'. In: *Pharmacognosy Review* 4(8) (2010), pp. 118–126. DOI: 10.4103/0973-7847.70902.

[42] Eric J Hall and Amato J Giaccia. *Radiobiology for the Radiologist*. 7th ed. Lippincott Williams & Wilkins, 2012. Chap. 2. ChoalepcteurlaTritMleechanisms of DNA and Chromosome Damage and Repair, pp. 12–34.

[43] Eric J Hall and Amato J Giaccia. *Radiobiology for the Radiologist*. 7th ed. Lippincott Williams & Wilkins, 2012. Chap. 7. Linear Energy Transfer and Relative Biologic Effectiveness, pp. 104–113.

[44] Eric J Hall and Amato J Giaccia. *Radiobiology for the Radiologist*. 7th ed. Lippincott Williams & Wilkins, 2012. Chap. 6. Oxygen Effect and Reoxygenation, pp. 86–103.

[45] Eric J Hall and Amato J Giaccia. *Radiobiology for the Radiologist*. 7th ed. Lippincott Williams & Wilkins, 2012. Chap. 3. Cell Survival Curves, pp. 35–66.

[46] JB Little. *Principal cellular and tissue effects of radiation*. 2003.

[47] Danielle Glick, Sandra Barth and Kay F Macleod. 'Autophagy: cellular and molecular mechanisms'. In: *The Journal of pathology* 221.1 (2010), pp. 3–12. DOI: 10.1002/path.2697.

[48] Popi Syntichaki and Nektarios Tavernarakis. 'Death by necrosis'. In: *EMBO reports* 3.7 (2002), pp. 604–609. DOI: 10.1093/embo-reports/kvf138.

[49] Nature. *Senescence articles from across Nature Portfolio*. URL: https://www.nature.com/subjects/senescence (visited on 14th June 2023).

[50] Christoph Richter, Jeen-Woo Park and Bruce N Ames. 'Normal oxidative damage to mitochondrial and nuclear DNA is extensive.' In: *Proceedings of the National Academy of Sciences* 85.17 (1988), pp. 6465–6467. DOI: 10.1073/pnas.85.17.6465.

[51] David A Clayton, Jackie N Doda and Errol C Friedberg. 'The absence of a pyrimidine dimer repair mechanism in mammalian mitochondria'. In: *Proceedings of the National Academy of Sciences* 71.7 (1974), pp. 2777–2781. DOI: 10.1073/pnas.71.7.277.

[52] Robert A Lansman and David A Clayton. 'Selective nicking of mammalian mitochondrial DNA in vivo: photosensitization by incorporation of 5-bromodeoxyuridine'. In: *Journal of Molecular Biology* 99.4 (1975), pp. 761–776. DOI: 10.1016/S0022-2836(75)80183-5.

[53] Stephen WG Tait and Douglas R Green. 'Mitochondrial regulation of cell death'. In: *Cold Spring Harbor perspectives in biology* 5.9 (2013), a008706. DOI: 10.1101/cshperspect.a008706.

[54] Eric J Hall and Amato J Giaccia. *Radiobiology for the Radiologist*. 7th ed. Lippincott Williams & Wilkins, 2012. Chap. 26. The Biology and Exploitation of Tumor Hypoxia, pp. 432–447.

[55] SR McKeown. 'Defining normoxia, physoxia and hypoxia in tumours—implications for treatment response'. In: *The British journal of radiology* 87.1035 (2014), p. 20130676. DOI: 10.1259/bjr.20130676.

[56] Bing-Hua Jiang et al. 'Hypoxia-inducible factor 1 levels vary exponentially over a physiologically relevant range of O2 tension'. In: *American Journal of Physiology-Cell Physiology* 271.4 (1996), pp. C1172–C1180. DOI: 10.1152/ajpcell.1996.271.4.C1172.

[57] Sharon La Fontaine and Julian FB Mercer. 'Trafficking of the copper-ATPases, ATP7A and ATP7B: role in copper homeostasis'. In: *Archives of biochemistry and biophysics* 463.2 (2007), pp. 149–167. DOI: 10.1016/j.abb.2007.04.021.

[58] Libre Texts Chemistry. *Oxidation-Reduction Reactions*. URL: https://chem.libretexts.org/Bookshelves/Analytical_Chemistry/Supplemental_Modules_(Analytical_Chemistry)/Electrochemistry/Redox_Chemistry/Oxidation-Reduction_Reactions (visited on 27th Apr. 2023).

[59] Carine White et al. 'Copper transport into the secretory pathway is regulated by oxygen in macrophages'. In: *Journal of cell science* 122.9 (2009), pp. 1315–1321. DOI: 10.1242/jcs.043216.

[60] Falk Martin et al. 'Copper-dependent activation of hypoxia-inducible factor (HIF)-1: implications for ceruloplasmin regulation'. In: *Blood* 105.12 (2005), pp. 4613–4619. DOI: 10.1182/blood-2004-10-3980.

[61] Fangyu Peng et al. 'PET of human prostate cancer xenografts in mice with increased uptake of 64CuCl2'. In: *Journal of Nuclear Medicine* 47.10 (2006), pp. 1649–1652.

[62] Cristina Ferrari et al. 'Copper-64 dichloride as theranostic agent for glioblastoma multiforme: a preclinical study'. In: *BioMed research international* 2015 (2015). DOI: 10.1155/2015/129764.

[63] Huawei Cai et al. 'Reduced 64Cu uptake and tumor growth inhibition by knockdown of human copper transporter 1 in xenograft mouse model of prostate cancer'. In: *Journal of Nuclear Medicine* 55.4 (2014), pp. 622–628. DOI: 10.2967/jnumed.113.126979.

[64] Chunxia Qin et al. 'Theranostics of malignant melanoma with 64CuCl2'. In: *Journal of Nuclear Medicine* 55.5 (2014), pp. 812–817. DOI: 10.2967/jnumed.113.133850.

[65] Mathilde Colombié et al. 'Focus on the controversial aspects of 64Cu-ATSM in tumoral hypoxia mapping by PET imaging'. In: *Frontiers in medicine* 2 (2015), p. 58. DOI: 10.3389/fmed.2015.00058.

[66] Atsushi Obata et al. 'Retention mechanism of hypoxia selective nuclear imaging/radiotherapeutic agent Cu-diacetyl-bis (N 4-methylthiosemicarbazone)(Cu-ATSM) in tumor cells'. In: *Annals of nuclear medicine* 15 (2001), pp. 499–504. DOI: 10.1007/BF02988502.

[67] Shahin Ramazi and Javad Zahiri. 'Post-translational modifications in proteins: resources, tools and prediction methods'. In: *Database* 2021 (2021). DOI: 10.1093/database/baab012.

[68] Fatima Ardito et al. 'The crucial role of protein phosphorylation in cell signaling and its use as targeted therapy'. In: *International journal of molecular medicine* 40.2 (2017), pp. 271–280. DOI: 10.3892/ijmm.2017.3036.

[69] Zhenfang Du and Christine M Lovly. 'Mechanisms of receptor tyrosine kinase activation in cancer'. In: *Molecular cancer* 17 (2018), pp. 1–13. DOI: 10.1186/s12943-018-0782-4.

[70] Dan R Robinson, Yi-Mi Wu and Su-Fang Lin. 'The protein tyrosine kinase family of the human genome'. In: *Oncogene* 19.49 (2000), pp. 5548–5557. DOI: 10.1038/sj.onc.1203957.

[71] GeeksforGeeks. *Receptor Tyrosine Kinase Signaling*. URL: https://www.geeksforgeeks.org/receptor-tyrosine-kinase-signaling/ (visited on 21st Feb. 2023).

[72] Richard Sever and Joan S Brugge. 'Signal transduction in cancer'. In: *Cold Spring Harbor perspectives in medicine* 5.4 (2015), a006098. DOI: 10.1101/cshperspect.a006098.

[73] Mihwa Kim, Minwoo Baek and Dae J Kim. 'Protein tyrosine signaling and its potential therapeutic implications in carcinogenesis'. In: *Current pharmaceutical design* 23.29 (2017), pp. 4226–4246. DOI: 10.2174/1381612823666170616082125.

[74] Philip Cohen, Darren Cross and Pasi A Jänne. 'Kinase drug discovery 20 years after imatinib: progress and future directions'. In: *Nature reviews drug discovery* 20.7 (2021), pp. 551–569. DOI: 10.1038/s41573-021-00195-4.

[75] Charles Pottier et al. 'Tyrosine kinase inhibitors in cancer: breakthrough and challenges of targeted therapy'. In: *Cancers* 12.3 (2020), p. 731. DOI: 10.3390/cancers12030731.

[76] Liling Huang, Shiyu Jiang and Yuankai Shi. 'Tyrosine kinase inhibitors for solid tumors in the past 20 years (2001–2020)'. In: *Journal of hematology & oncology* 13 (2020), pp. 1–23. DOI: 10.1186/s13045-020-00977-0.

[77] Nicholas Borcherding et al. 'ROR1, an embryonic protein with an emerging role in cancer biology'. In: *Protein & cell* 5.7 (2014), pp. 496–502. DOI: 10.1007/s13238-014-0059-7.

[78] Yan Liu et al. 'Wnt5a induces homodimerization and activation of Ror2 receptor tyrosine kinase'. In: *Journal of cellular biochemistry* 105.2 (2008), pp. 497–502. DOI: 10.1002/jcb.21848.

[79] Michael P O'Connell et al. 'Hypoxia Induces Phenotypic Plasticity and Therapy Resistance in Melanoma via the Tyrosine Kinase Receptors ROR1 and ROR2ROR1 and ROR2 in Invasion and Therapy Resistance'. In: *Cancer discovery* 3.12 (2013), pp. 1378–1393. DOI: 10.1158/2159-8290.CD-13-0005.

[80] Brian A Hemmings and David F Restuccia. 'Pi3k-pkb/akt pathway'. In: *Cold Spring Harbor perspectives in biology* 4.9 (2012), a011189. DOI: 10.1101/cshperspect.a011189.

[81] Vincent T Bicocca et al. 'Crosstalk between ROR1 and the Pre-B cell receptor promotes survival of t (1; 19) acute lymphoblastic leukemia'. In: *Cancer cell* 22.5 (2012), pp. 656–667. DOI: 10.1016/j.ccr.2012.08.027.

[82] Amir Hossein Daneshmanesh et al. 'The PI3K/AKT/mTOR pathway is involved in direct apoptosis of CLL cells induced by ROR1 monoclonal antibodies'. In: *British journal of haematology* 169.3 (2015), pp. 455–458. DOI: 10.1111/bjh.13228.

[83] Natalia Brenda Fernández et al. 'ROR1 contributes to melanoma cell growth and migration by regulating N-cadherin expression via the PI3K/Akt pathway'. In: *Molecular carcinogenesis* 55.11 (2016), pp. 1772–1785. DOI: 10.1002/mc.22426.

[84] Suping Zhang et al. 'ROR1 is expressed in human breast cancer and associated with enhanced tumor-cell growth'. In: *PloS one* 7.3 (2012), e31127. DOI: 10.1371/journal.pone.0031127.

[85] Bing Cui et al. 'Targeting ROR1 inhibits epithelial–mesenchymal transition and metastasis'. In: *Cancer research* 73.12 (2013), pp. 3649–3660. DOI: 10.1158/0008-5472.CAN-12-3832.

[86] Vignesh Sivaganesh et al. 'Inhibiting ROR1 expression in Androgen-Independent Prostate Cancer Reduces Aggressive Cancer Phenotypes by modulation of AKT-GSK3 Pathway'. In: (2021).

[87] Norman Fultang et al. 'ROR1 regulates chemoresistance in Breast Cancer via modulation of drug efflux pump ABCB1'. In: *Scientific reports* 10.1 (2020), pp. 1–12. DOI: 10.1038/s41598-020-58864-0.

[88] Yan-Jun Guo et al. 'ERK/MAPK signalling pathway and tumorigenesis'. In: *Experimental and therapeutic medicine* 19.3 (2020), pp. 1997–2007. DOI: 10.3892/etm.2020.8454.

[89] Hanna Karvonen et al. 'Wnt5a and ROR1 activate non-canonical Wnt signaling via RhoA in TCF3-PBX1 acute lymphoblastic leukemia and highlight new treatment strategies via Bcl-2 co-targeting'. In: *Oncogene* 38.17 (2019), pp. 3288–3300. DOI: 10.1038/s41388-018-0670-9.

[90] Jiadong Li et al. 'Stat3 signaling pathway: a future therapeutic target for bone-related diseases'. In: *Frontiers in Pharmacology* 13 (2022). DOI: 10.3389/fphar.2022.897539.

[91] Yun Chen et al. 'Cirmtuzumab blocks Wnt5a/ROR1 stimulation of NF-$\kappa$B to repress autocrine STAT3 activation in chronic lymphocytic leukemia'. In: *Blood, The Journal of the American Society of Hematology* 134.13 (2019), pp. 1084–1094. DOI: 10.1182/blood.2019001366.

[92] Ting Liu et al. 'NF-$\kappa$B signaling in inflammation'. In: *Signal transduction and targeted therapy* 2.1 (2017), pp. 1–9. DOI: 10.1038/sigtrans.2017.23.

[93] Ulf Klein et al. 'Gene expression profiling of B cell chronic lymphocytic leukemia reveals a homogeneous phenotype related to memory B cells'. In: *The Journal of experimental medicine* 194.11 (2001), pp. 1625–1638. DOI: 10.1084/jem.194.11.1625.

[94] Amir Hossein Daneshmanesh et al. 'Orphan receptor tyrosine kinases ROR1 and ROR2 in hematological malignancies'. In: *Leukemia & lymphoma* 54.4 (2013), pp. 843–850. DOI: 10.3109/10428194.2012.731599.

[95] Bing Cui et al. 'High-level ROR1 associates with accelerated disease progression in chronic lymphocytic leukemia'. In: *Blood, The Journal of the American Society of Hematology* 128.25 (2016), pp. 2931–2940. DOI: 10.1182/blood-2016-04-712562.

[96] Jian-Kang Zhou et al. 'ROR1 expression as a biomarker for predicting prognosis in patients with colorectal cancer'. In: *Oncotarget* 8.20 (2017), p. 32864. DOI: 10.18632/oncotarget.15860.

[97] Huilin Zhang et al. 'ROR1 expression correlated with poor clinical outcome in human ovarian cancer'. In: *Scientific reports* 4.1 (2014), p. 5811. DOI: 10.1038/srep05811.

[98] F Klemm et al. '$\beta$-catenin-independent WNT signaling in basal-like breast cancer and brain metastasis'. In: *Carcinogenesis* 32.3 (2011), pp. 434–442. DOI: 10.1093/carcin/bgq269.

[99] Takeshi Saji et al. 'Critical role of the ror-family of receptor tyrosine kinases in invasion and proliferation of malignant pleural mesothelioma cells'. In: *Genes to Cells* 23.7 (2018), pp. 606–613. DOI: 10.1111/gtc.12599.

[100] Jian Yu et al. 'Wnt5a induces ROR1/ROR2 heterooligomerization to enhance leukemia chemotaxis and proliferation'. In: *The Journal of clinical investigation* 126.2 (2016), pp. 585–598. DOI: 10.1172/JCI83535.

[101] Mohammad Hojjat-Farsangi et al. 'Inhibition of the receptor tyrosine kinase ROR1 by anti-ROR1 monoclonal antibodies and siRNA induced apoptosis of melanoma cells'. In: *PloS one* 8.4 (2013), e61167. DOI: 10.1371/journal.pone.0061167.

[102] Tomoya Yamaguchi et al. 'NKX2-1/TITF1/TTF-1-Induced ROR1 is required to sustain EGFR survival signaling in lung adenocarcinoma'. In: *Cancer cell* 21.3 (2012), pp. 348–361. DOI: 10.1016/j.ccr.2012.02.008.

[103] George F Widhopf et al. 'ROR1 can interact with TCL1 and enhance leukemogenesis in E$\mu$-TCL1 transgenic mice'. In: *Proceedings of the National Academy of Sciences* 111.2 (2014), pp. 793–798. DOI: 10.1073/pnas.130837411.

[104] Qi Zhou et al. 'Stable silencing of ROR1 regulates cell cycle, apoptosis, and autophagy in a lung adenocarcinoma cell line'. In: *International Journal of Clinical and Experimental Pathology* 13.5 (2020), p. 1108.

[105] Claire Henry et al. 'Targeting the ROR1 and ROR2 receptors in epithelial ovarian cancer inhibits cell migration and invasion'. In: *Oncotarget* 6.37 (2015), p. 40310. DOI: 10.18632/oncotarget.5643.

[106] Markéta Kaucká et al. 'Post-translational modifications regulate signalling by Ror1'. In: *Acta physiologica* 203.3 (2011), pp. 351–362. DOI: 10.1111/j.1748-1716.2011.02306.x.

[107] Michiru Nishita et al. 'Filopodia formation mediated by receptor tyrosine kinase Ror2 is required for Wnt5a-induced cell migration'. In: *The Journal of cell biology* 175.4 (2006), pp. 555–562. DOI: 10.1083/jcb.200607127.

[108] CE Henry et al. 'Migration and invasion is inhibited by silencing ROR1 and ROR2 in chemoresistant ovarian cancer'. In: *Oncogenesis* 5.5 (2016), e226–e226. DOI: 10.1038/oncsis.2016.32.

[109] Syed S Islam et al. 'Antibody-drug conjugate T-DM1 treatment for HER2+ breast cancer induces ROR1 and confers resistance through activation of Hippo transcriptional coactivator YAP1'. In: *EBioMedicine* 43 (2019), pp. 211–224. DOI: 10.1016/j.ebiom.2019.04.061.

[110] Suping Zhang et al. 'Inhibition of chemotherapy resistant breast cancer stem cells by a ROR1 specific antibody'. In: *Proceedings of the National Academy of Sciences* 116.4 (2019), pp. 1370–1377. DOI: 10.1073/pnas.1816262116.

[111] Hanna Karvonen et al. 'Molecular mechanisms associated with ROR1-mediated drug resistance: crosstalk with Hippo-YAP/TAZ and BMI-1 pathways'. In: *Cells* 8.8 (2019), p. 812. DOI: 10.3390/cells8080812.

[112] Tetsuya Fukuda et al. 'Antisera induced by infusions of autologous Ad-CD154-leukemia B cells identify ROR1 as an oncofetal antigen and receptor for Wnt5a'. In: *Proceedings of the National Academy of Sciences* 105.8 (2008), pp. 3047–3052. DOI: 10.1073/pnas.0712148105.

[113] Richa Karmakar. 'State of the art of bacterial chemotaxis'. In: *Journal of Basic Microbiology* 61.5 (2021), pp. 366–379. DOI: 10.1002/jobm.202000661.

[114] Tomohiro Ishikawa et al. 'Ror1 is expressed inducibly by Notch and hypoxia signaling and regulates stem cell-like property of glioblastoma cells'. In: *Cancer Science* (2022). DOI: 10.1111/cas.15630.

[115] Excedr. *Cell Lysate: Overview Applications*. URL: https://www.excedr.com/resources/cell-lysate/ (visited on 30th Mar. 2023).

[116] Svea Matthiesen, Rico Jahnke and Michael R Knittler. 'A straightforward hypoxic cell culture method suitable for standard incubators'. In: *Methods and Protocols* 4.2 (2021), p. 25. DOI: 10.3390/mps4020025.

[117] Carlos HV Nascimento-Filho et al. 'From Tissue Physoxia to Cancer Hypoxia, Cost-Effective Methods to Study Tissue-Specific O2 Levels in Cellular Biology'. In: *International Journal of Molecular Sciences* 23.10 (2022), p. 5633. DOI: 10.3390/ijms23105633.

[118] Danli Wu and Patricia Yotnda. 'Induction and testing of hypoxia in cell culture'. In: *JoVE (Journal of Visualized Experiments)* 54 (2011), e2899. DOI: 10.3791/2899.

[119] Samuel B Bader, Mark W Dewhirst and Ester M Hammond. 'Cyclic hypoxia: an update on its characteristics, methods to measure it and biological implications in cancer'. In: *Cancers* 13.1 (2020), p. 23. DOI: 10.3390/cancers13010023.

[120] Kritika Saxena and Mohit Kumar Jolly. 'Acute vs. chronic vs. cyclic hypoxia: their differential dynamics, molecular mechanisms, and effects on tumor progression'. In: *Biomolecules* 9.8 (2019), p. 339. DOI: 10.3390/biom9080339.

[121] Yanchun Liu et al. 'Silencing of receptor tyrosine kinase ROR1 inhibits tumor-cell proliferation via PI3K/AKT/mTOR signaling pathway in lung adenocarcinoma'. In: *PloS one* 10.5 (2015), e0127092. DOI: 10.1371/journal.pone.0127092.

[122] ThermoFisher Scientific. *RNA interference (RNAi) is an evolutionarily conserved mechanism for silencing gene expression.* URL: https://www.thermofisher.com/no/en/home/references/ambion-tech-support/rnai-sirna/tech-notes/duration-of-sirna-induced-silencing.html (visited on 8th June 2023).

[123] Erin P O'Keefe. 'siRNAs and shRNAs: Tools for protein knockdown by gene silencing'. In: *Materials and Methods* 3 (2013). DOI: 10.13070/mm.en.3.197.

[124] Tahrin Mahmood, Ping-Chang Yang et al. 'Western blot: technique, theory, and trouble shooting'. In: *North American journal of medical sciences* 4.9 (2012), p. 429. DOI: 10.4103/1947-2714.100998.

[125] Mauricio Rocha-Martins, Brian Njaine and Mariana S Silveira. 'Avoiding pitfalls of internal controls: validation of reference genes for analysis by qRT-PCR and Western blot throughout rat retinal development'. In: (2012). DOI: 10.1371/journal.pone.0043028.

[126] Cherie L Butts and Esther M Sternberg. 'Flow cytometry as a tool for measurement of steroid hormone receptor protein expression in leukocytes'. In: *The Nuclear Receptor Superfamily: Methods and Protocols* (2009), pp. 35–50. DOI: 10.1007/978-1-60327-575-0_3.

[127] Cell Signaling Technology. *When should I use flow cytometry for signaling instead of western blot?* URL: https://blog.cellsignal.com/when-should-i-use-flow-cytometry-for-signaling-instead-of-western-blot (visited on 9th June 2023).

[128] Maimon E Hubbi et al. 'A nontranscriptional role for HIF-1$\alpha$ as a direct inhibitor of DNA replication'. In: *Science signaling* 6.262 (2013), ra10–ra10. DOI: 10.1126/scisignal.2003417.

[129] Heather Nesbitt et al. 'Targeting Hypoxic Prostate Tumors Using the Novel Hypoxia-Activated Prodrug OCT1002 Inhibits Expression of Genes Associated with Malignant ProgressionOCT1002 Inhibits Malignant Progression of Hypoxic Tumors'. In: *Clinical Cancer Research* 23.7 (2017), pp. 1797–1808. DOI: 10.1158/1078-0432.CCR-16-1361.

[130] Yao Dai, Kyungmi Bae and Dietmar W Siemann. 'Impact of hypoxia on the metastatic potential of human prostate cancer cells'. In: *International Journal of Radiation Oncology* Biology* Physics* 81.2 (2011), pp. 521–528. DOI: 10.1016/j.ijrobp.2011.04.027.

[131] Yingchun Tang et al. 'Hypoxia enhances activity and malignant behaviors of colorectal cancer cells through the STAT3/MicroRNA-19a/PTEN/PI3K/AKT axis'. In: *Analytical Cellular Pathology* 2021 (2021), pp. 1–19. DOI: 10.1155/2021/4132488.

[132] Leslimar Rios-Colon et al. 'Carnitine palmitoyltransferase 1 regulates prostate cancer growth under hypoxia'. In: *Cancers* 13.24 (2021), p. 6302. DOI: 10.3390/cancers13246302.

[133] LH Higgins et al. 'Hypoxia and the metabolic phenotype of prostate cancer cells'. In: *Biochimica et Biophysica Acta (BBA)-Bioenergetics* 1787.12 (2009), pp. 1433–1443. DOI: 10.1016/j.bbabio.2009.06.003.

[134] Xiaolu Li et al. 'Lactate metabolism in human health and disease'. In: *Signal Transduction and Targeted Therapy* 7.1 (2022), p. 305. DOI: 10.1038/s41392-022-01151-3.

[135] Encouse B Golden et al. 'The convergence of radiation and immunogenic cell death signaling pathways'. In: *Frontiers in oncology* 2 (2012), p. 88. DOI: 10.3389/fonc.2012.00088.

[136] abcam. *MTS Assay Kit (Cell Proliferation) (Colorimetric) (ab197010).* URL: https://www.abcam.com/products/assay-kits/mts-assay-kit-cell-proliferation-colorimetric-ab197010.html (visited on 8th June 2023).

[137] Amineh Ghaderi et al. 'A Small Molecule Targeting the Intracellular Tyrosine Kinase Domain of ROR1 (KAN0441571C) Induced Significant Apoptosis of Non-Small Cell Lung Cancer (NSCLC) Cells'. In: *Pharmaceutics* 15.4 (2023), p. 1148. DOI: 10.3390/pharmaceutics15041148.

[138] Amir H DaneshManesh et al. 'Ror1, a cell surface receptor tyrosine kinase is expressed in chronic lymphocytic leukemia and may serve as a putative target for therapy'. In: *International journal of cancer* 123.5 (2008), pp. 1190–1195. DOI: 10.1002/ijc.23587.

[139] Dongli Liu et al. 'ROR1 is upregulated in endometrial cancer and represents a novel therapeutic target'. In: *Scientific Reports* 10.1 (2020), pp. 1–13. DOI: 10.1038/s41598-020-70924-z.

[140] Sivasubramanian Baskar et al. 'Unique cell surface expression of receptor tyrosine kinase ROR1 in human B-cell chronic lymphocytic leukemia'. In: *Clinical Cancer Research* 14.2 (2008), pp. 396–404. DOI: 10.1158/1078-0432.CCR-07-1823.

[141] Brian S Cummings and Rick G Schnellmann. 'Measurement of cell death in mammalian cells'. In: *Current protocols in pharmacology* 25.1 (2004), pp. 12–8. DOI: 10.1002/0471141755.ph1208s25.

[142] Noboru Mizushima, Tamotsu Yoshimori and Beth Levine. 'Methods in mammalian autophagy research'. In: *Cell* 140.3 (2010), pp. 313–326. DOI: 10.1016/j.cell.2010.01.028.

[143] Translational Research Institute University of Arkansas for Medical Sciences. *What is Translational Research?* URL: https://tri.uams.edu/about-tri/ (visited on 14th June 2023).

[144] John M Buatti and Ana P Kiess. 'The rapid evolution of theranostics in radiation oncology'. In: *Seminars in radiation oncology*. Vol. 31. 1. Elsevier. 2021, pp. 1–2. DOI: 10.1016/j.semradonc.2020.07.001.

[145] Torjan Haslerud and Mona-Elisabeth R Revheim. 'Therapeutics+ diagnostics= theranostics'. In: *Tidsskrift for Den norske legeforening* (2023). DOI: 10.4045/tidsskr.22.0776.

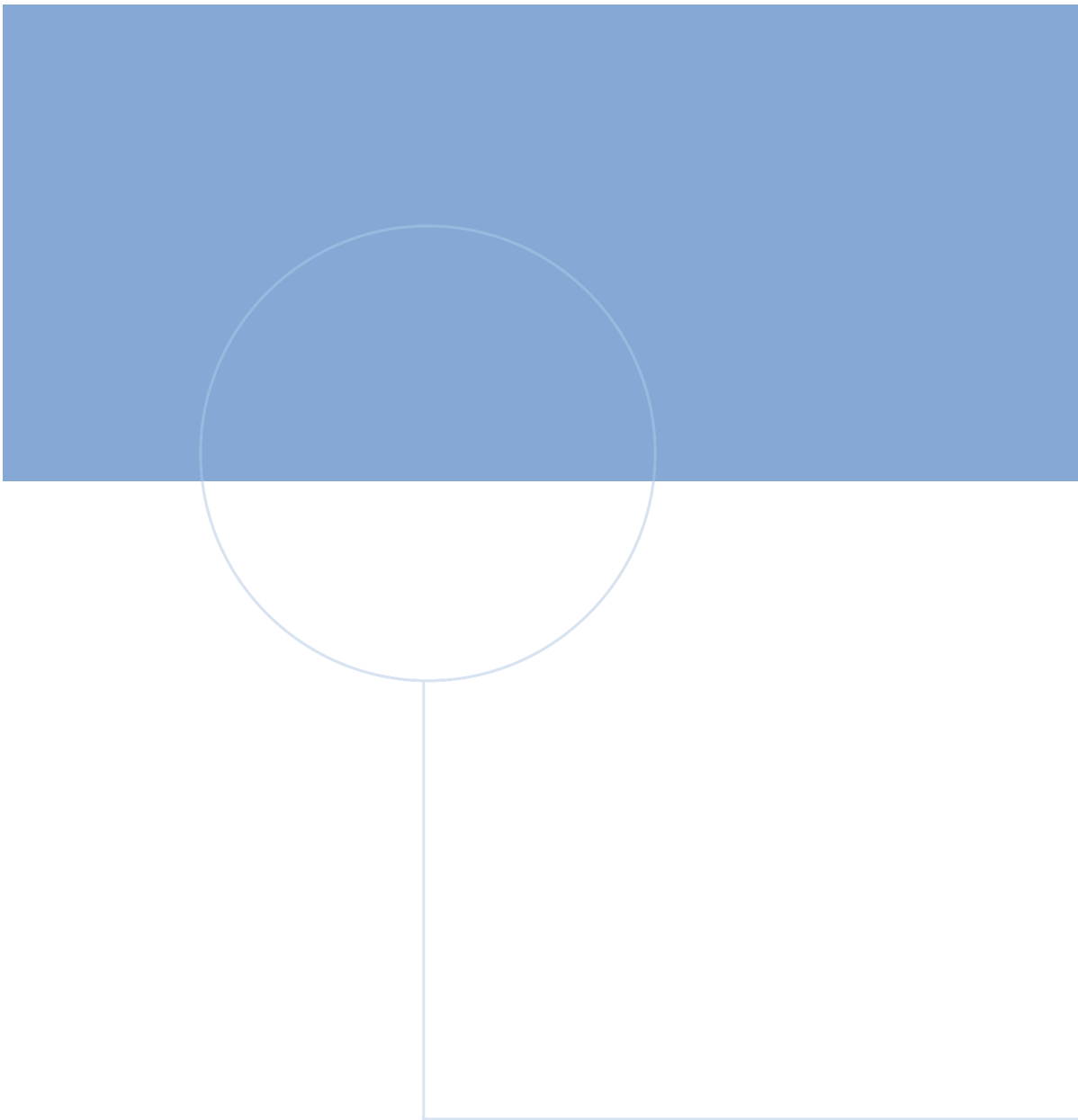

NTNU

Norwegian University of
Science and Technology